OPEN ACCESS
IOP Publishing
Journal of Physics G: Nuclear and Particle Physics
J. Phys. G: Nucl. Part. Phys. **44** (2017) 105201 (35pp)
https://doi.org/10.1088/1361-6471/aa84da

Calculation of the decay rate of tachyonic neutrinos against charged-lepton-pair and neutrino-pair Cerenkov radiation

Ulrich D Jentschura[1,2], István Nándori[3] and Robert Ehrlich[2]

[1] Department of Physics, Missouri University of Science and Technology, Rolla, MO65409, United States of America
[2] MTA–DE Particle Physics Research Group, PO Box 51, H-4001 Debrecen, Hungary
[3] Department of Physics, George Mason University, Fairfax, VA 22030, United States of America

E-mail: ulj@mst.edu

Received 5 April 2017
Accepted for publication 8 August 2017
Published 12 September 2017

Abstract

We consider in detail the calculation of the decay rate of high-energy superluminal neutrinos against (charged) lepton pair Cerenkov radiation, and neutrino pair Cerenkov radiation, i.e., against the decay channels $\nu \to \nu\, e^+\, e^-$ and $\nu \to \nu\, \overline{\nu}\, \nu$. Under the hypothesis of a tachyonic nature of neutrinos, these decay channels put constraints on the lifetime of high-energy neutrinos for terrestrial experiments as well as on cosmic scales. For the oncoming neutrino, we use the Lorentz-covariant tachyonic relation $E_\nu = \sqrt{\vec{p}^{\,2} - m_\nu^2}$, where m_ν is the tachyonic mass parameter. We derive both threshold conditions as well as on decay and energy loss rates, using the plane-wave fundamental bispinor solutions of the tachyonic Dirac equation. Various intricacies of rest frame versus lab frame calculations are highlighted. The results are compared to the observations of high-energy IceCube neutrinos of cosmological origin.

Keywords: neutrinos, tachyons, generalized Dirac equations, decay processes, Lorentz invariance

(Some figures may appear in colour only in the online journal)

1. Introduction

We describe a calculation of the decay rate and energy loss rate of tachyonic (superluminal, 'faster-than-light') neutrinos due to (charged) lepton pair Cerenkov radiation (LPCR) and neutrino pair Cerenkov radiation (NPCR). These two decay channels proceed via virtual Z^0 bosons. The processes are kinematically allowed for tachyonic (space-like) neutrinos, and in the case of LPCR, above a certain energy threshold dependent on the neutrino mass. We base our treatment on a Lorentz-covariant theory of tachyonic (faster-than-light) spin-$1/2$ particles, i.e., on the tachyonic Dirac (not Majorana) equation [1–5]. Solutions of this equation [6–10] fulfill the Lorentz-covariant dispersion relation $E = (\vec{k}^2 - m_\nu^2)^{1/2}$, where E is the energy and $\vec{k}$ is the spatial momentum vector, while m_ν is the tachyonic parameter, corresponding to a negative Lorentz-invariant mass square $-m_\nu^2$. The quantity $p^\mu\, p_\mu = E^2 - \vec{k}^2 = -m_\nu^2$ is Lorentz-invariant. (Again, we shall assume here that neutrinos are Dirac particles and use the tachyonic Dirac equation [1–5] as a candidate for their physical description.)

Tachyonic kinematics are somewhat counter-intuitive. For example, tachyons accelerate as they lose energy. For a subluminal ('tardyonic') particle, one can perform a Lorentz transformation into the rest frame where the spatial momentum k' of the particle vanishes. For a tachyonic particle, one can show that, starting from a state with real (as opposed to complex) energy $\sqrt{k^2 - m_\nu^2}$, that the Lorentz-transformed momentum always remains greater or equal than than m_ν, i.e., $k' \geqslant m_\nu$, and the Lorentz-transformed energy E' remains real [10]. One thus cannot possibly enter the rest frame where otherwise we would have $k' = 0$, and the energy would become complex. All that we can do for a tachyon is to transform into a frame where the Lorentz-transformed energy of the neutrino vanishes, i.e., we can enforce $E' = 0$, but not $k' = 0$. The latter frame constitutes a (distant) analog of the 'rest frame' of a tachyonic particle, where according to the classical dispersion relation, the fact that $E = m_\nu \Big/ \sqrt{v_\nu^2 - 1} = 0$ otherwise implies an infinite velocity $v_\nu = \infty$. All of these intricacies have to be taken into account in the calculation of threshold conditions and decay rates.

Here, we analyze the decay of energetic tachyonic neutrino via LPCR and NPCR. In the calculation of the decay and energy loss rates, we make extensive use of a recently developed formalism which expresses the solutions of the tachyonic Dirac equation in terms of helicity spinors [6–10]. Indeed, helicity remains a good quantum number for tachyonic solutions while the chirality operator does not commute with the tachyonic Dirac Hamiltonian, a fact which, among other things, leads to a natural explanation for the $V - A$ structure of the weak leptonic current [11]. On a different issue, in particle physics, one usually carries out sums over the bispinor solutions using Casimir's trick [12], which is based on sum formulas that allow one to express the sum over the spin orientations of the spin-$1/2$ in a very concise, analytic form. For the tachyonic Dirac equation, the analogous sum formulas have recently been found [6, 9], in the helicity basis.

A further complication arises because the time ordering along a space-like trajectory of a tachyonic neutrino is not unique. For a straight space-like trajectory with velocity $v_\nu > c$, it is possible to boost into a system with velocity $u = c^2/v_\nu$, where the tachyonic particle assumes an infinite velocity, according to the velocity addition theorem $v' = (v_\nu - u)/(1 - u\, v_\nu/c^2)$. Because $v_\nu > c$, we still have $u = c^2/v_\nu < c$, which makes the boost permissible. A boost into any frame with velocity u' (with $u < u' < c$) will reverse the time ordering along a tachyonic trajectory. The time ordering problem for a tachyonic trajectory is connected with the problem that some fundamental tachyonic particle operators necessarily transform into tachyonic antiparticle operators upon Lorentz transformation [13–21]. For the decay of a tachyonic neutrino into an electron–positron pair, this consideration implies that one is at risk

of picking up a contribution from neutrino–antineutrino annihilation when considering the decay of an incoming tachyonic neutrino. One can avoid this pitfall by introducing helicity projectors; these eliminate the spurious contribution from the annihilation channel. A clear exposition of the underlying formalism is one of the purposes of the current investigation.

The observation of highly energetic cosmic neutrinos by the IceCube collaboration [22–24] puts constraints on the superluminality of neutrinos because they need to 'survive' the decay processes $\nu \to \nu e^+ e^-$ and $\nu \to \nu\, \overline{\nu}\, \nu$. So, if the decay rate is otherwise sufficiently large in order to account for a substantial energy loss on interstellar time and distance scales, then one may relate the tachyonic threshold to a conceivable high-energy cutoff of the cosmic neutrino spectrum at a threshold energy $E = E_{\rm th} \approx 2$ PeV [22–24]. Namely, in principle (see [25]), the tachyonic theory allows us to express the threshold energy as a function of the electron and neutrino masses, $E_{\rm th} = f(m_e, m_\nu)$; a specific value of the threshold thus implies a definite value of m_ν and also determines a numerical value for $\delta_\nu = v_\nu^2/c^2 - 1$, because of the dispersion relation $E = m_\nu/\delta_\nu^{1/2}$. However, all these conjectures crucially depend on the overall magnitude of the decay and energy loss rates: if these should turn out to be negligible on cosmic distance and time scales, then it will be impossible to relate the tachyonic mass parameter to the cutoff; hence, it is very important to have explicit results for the decay rates at hand.

We here continue a series of investigations, continued over the last decades, on tachyonic particles [13, 15–18, 26, 27] in general and spin-1/2 particles and the superluminal neutrino hypothesis in particular [1, 19–21, 28–30]. The latter include Lorentz-violating models [31–38] which lead to superluminality; such models have been applied to the analysis of astrophysical data [39, 40]. Energy loss mechanisms due to LPCR have been subjected to alternative statistical analyses [41], and compared to other energy loss mechanisms, e.g., due to neutrino splitting [42]. Neutrino speed modifications have been linked to conceivable (local) variations in fundamental constants [43], and a connection of neutrino speed and neutrino flavor oscillations has been highlighted in [44]. Gravitational interactions have also been linked to neutrino speed modifications [45, 46]. In terms of conceptual questions underlying both spinless as well as spin-1/2 tachyonic theories, including the stability of the vacuum, we refer to the discussion in [9, 47]. A lengthy further discussion on the conceptual issues underlying the tachyonic model would otherwise be beyond the current paper, which already is quite verbose.

We organize our investigations as follows. In section 2, we derive the energy threshold for LPCR as a function of the tachyonic mass parameter m_ν. The derivation of the decay and energy loss rates due to LPCR is described in section 3. For NPCR, formulas can be found in section 4. Phenomenological consequences (IceCube data) are discussed in section 5. Units with $\hbar = c = \epsilon_0 = 1$ are used throughout this paper.

2. Thresholds, Fermi theory and tachyonic decays

2.1. Tachyonic lepton pair threshold based on a space-like dispersion relation

We consider the process shown in figure 1(a), which is LPCR. The threshold condition reads as $q^2 = (E_3 - E_1)^2 - (\vec{k}_3 - \vec{k}_1)^2 \geqslant 4m_e^2$, where q is the four-momentum of the virtual Z^0 boson, while the incoming and outgoing neutrino momenta are $p_1^\mu = (E_1, \vec{k}_1)$ and $p_3^\mu = (E_3, \vec{k}_3)$. Threshold is reached when, depending on the geometry, the energy transfer from initial to final state is maximum, while the spatial momentum transfer is minimum. This implies that a larger spatial momentum transfer actually is disfavored from a point of view of

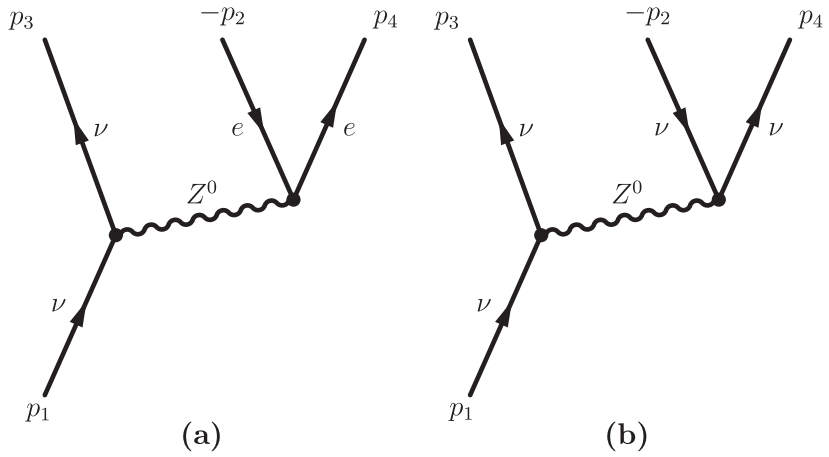

Figure 1. The incoming and outgoing momenta, for lepton pair Cerenkov radiation (LPCR), from a tachyonic neutrino, are used as indicated in the Feynman diagram (a). The arrow of time is from bottom to top. The four-momentum of the incoming highly energetic superluminal neutrino carries a subscript 1; it decays into a neutrino of lesser energy (subscript 3), while producing an electron–positron pair (subscripts 2 and 4). In figure (b), the decay products are tachyonic neutrinos of the same mass eigenstate as the oncoming one. The depicted process is referred to as neutrino-pair Cerenkov radiation (NPCR).

pair production, because it leads to lesser values of q^2. In other words, the greater the spatial momentum transfer, the smaller is the four-momentum transfer. Geometrically, we want the outgoing spatial momentum to be as close to the incoming spatial momentum as possible. At threshold, we can thus safely assume that the final neutrino state actually propagates into the same direction as the initial state.

Threshold is reached for a collinear geometry of maximum symmetry. The incoming and outgoing tachyonic particles are on the mass shell, i.e., $E_1 = \sqrt{k_1^2 - m_\nu^2}$ and $E_3 = \sqrt{k_3^2 - m_\nu^2}$. The four-vector notation can thus be reduced to just two components, $q = (E_3, k_3) - (E_1, k_1)$, and the momentum transfer q^2 carried by the Z^0 boson therefore reads as follows,

$$q^2 = (E_1 - E_3)^2 - (k_1 - k_3)^2. \tag{2.1}$$

Electron–positron pair production threshold is reached at

$$q^2 = (\sqrt{k_1^2 - m_\nu^2} - \sqrt{k_3^2 - m_\nu^2})^2 - (k_1 - k_3)^2 = 4m_e^2. \tag{2.2}$$

For minimum energy and momentum of the final neutrino state, we have $E_3 = 0$ and $k_3 = m_\nu$. Then, the condition (2.2) transforms into

$$(k_1)_{\rm th} = 2\frac{m_e^2}{m_\nu} + m_\nu. \tag{2.3}$$

The energy of the tachyonic neutrino at threshold is given as

$$(E_1)_{\rm th} = \sqrt{(k_1)_{\rm th}^2 - m_\nu^2} = 2\,\frac{m_e}{m_\nu}\,\sqrt{m_e^2 + m_\nu^2} \approx 2\,\frac{m_e^2}{m_\nu} + m_\nu + \mathcal{O}\left(\frac{m_\nu^3}{m_e^2}\right), \tag{2.4}$$

where the latter approximation is valid for $\delta \ll 1$. One can rewrite this result, based on the tachyonic dispersion relation $m_\nu = E_1 \sqrt{v_\nu^2 - 1} = E_1 \sqrt{\delta_\nu}$,

$$(E_1)_{\rm th} \approx (k_1)_{\rm th} = 2\frac{m_e^2}{m_\nu} + m_\nu \approx 2\frac{m_e^2}{m_\nu} = 2\frac{m_e^2}{(E_1)_{\rm th}\sqrt{\delta_\nu}} \;\Rightarrow\; (E_1)_{\rm th} \approx \sqrt{2}\,\frac{m_e}{\delta_\nu^{1/4}}. \tag{2.5}$$

We note that the tachyonic threshold is a definite function of the mass parameters m_ν and m_e of the tachyonic neutrino and of the electron (positron), respectively.

2.2. Tachyonic neutrino pair threshold based on a space-like dispersion relation

In the previous section, we found that for electron–positron (charged lepton) pair production, threshold is reached for a collinear geometry. In order to investigate the presence or absence of a threshold for tachyonic pair production (i.e, with two outgoing tachyons), it is instructive to have a look at various geometries. Let us consider a pair of tachyons, both of them on the mass shell, $E^2 - \vec{k}^2 = -m_\nu^2$. The outgoing particles of the pair are labeled with the indices 2 and 4, as in figure 1. If we assume that the tachyons are emitted collinearly and with the same energy, then $p^\mu = (E, \vec{k}) = p_2^\mu = (E_2, \vec{k}_2) = p_4^\mu = (E_4, \vec{k}_4)$, and

$$q^2 = (p_2 + p_4)^2 = 4p^\mu p_\mu = 4\,(\vec{k}^2 - m_\mu^2) - 4\,\vec{k}^2 = -4\,m_\mu^2, \tag{2.6}$$

which is negative. For two neutrinos of different energy, emitted collinearly. i.e., with $\vec{k}_2 = k_2\,\hat{\rm e}_z$ and $\vec{k}_4 = k_4\,\hat{\rm e}_z$), one has

$$E_2 = \sqrt{k_2^2 - m_\mu^2}, \qquad E_4 = \sqrt{k_4^2 - m_\mu^2}, \tag{2.7a}$$

$$q^2 = (\sqrt{k_2^2 - m_\mu^2} + \sqrt{k_4^2 - m_\mu^2})^2 - (k_2 + k_4)^2. \tag{2.7b}$$

For small tachyonic mass parameter m_ν, a Taylor expansion yields

$$q^2 = -\left(2 + \frac{k_2}{k_4} + \frac{k_4}{k_2}\right) m_\nu^2 + \mathcal{O}(m_\nu^4). \tag{2.8}$$

In the limits $k_2 \to 0$, $k_4 \to \infty$ (or vice versa), q^2 assumes very large negative numerical values, demonstrating the absence of a lower threshold.

One might ask, however, if there is perhaps a higher cutoff for the allowed q^2 in relativistic tachyonic pair production kinematics. For the production of an anti-collinear pair, one has

$$\vec{k}_2 = k_2\,\hat{\rm e}_z, \qquad \vec{k}_4 = -k_4\,\hat{\rm e}_z, \tag{2.9a}$$

$$E_2 = \sqrt{k_2^2 - m_\mu^2}, \qquad E_4 = \sqrt{k_4^2 - m_\mu^2}, \tag{2.9b}$$

$$\begin{aligned} q^2 &= (\sqrt{k_2^2 - m_\mu^2} + \sqrt{k_4^2 - m_\mu^2})^2 - (k_2 - k_4)^2 \\ &= 4k_2k_4 + O(m_\nu^2). \end{aligned} \tag{2.9c}$$

For large k_1 and k_2, this expression assumes arbitrarily large positive numerical values. The only condition relevant to the allowed range of q^2 for tachyonic pair production thus is

$$-\infty < q^2 < \infty, \qquad q^0 > 0. \tag{2.10}$$

This result has important consequences for the calculation of neutrino-pair Cerenkov radiation (see figure 1(b)).

2.3. Tachyonic maximum momentum transfer and Fermi theory

One crucial question one might ask concerns the applicability of Fermi theory for the decay processes shown in figures 1(a) and (b), in the high-energy regime. The question is whether the condition $q^2 \ll M_Z^2$, which ensures the applicability of Fermi theory, remains valid for a highly energetic, oncoming neutrino. Concerning this question, we first recall that, as already shown, threshold for pair production is reached for collinear geometry, i.e., when the final neutrino momentum k_3 is along the same direction as the initial state momentum k_1. This implies that the maximum momentum transfer, for given energy E_1 of the incoming particle, also is reached for collinear geometry. Reducing space to one dimension, we find for the square q^2 of the momentum transfer,

$$\begin{aligned} q^2 &= (\sqrt{k_1^2 - m_\nu^2} - \sqrt{k_3^2 - m_\nu^2})^2 - (k_1 - k_3)^2 \\ &= 2(k_1 k_3 - \sqrt{k_1^2 - m_\nu^2}\,\sqrt{k_3^2 - m_\nu^2} - m_\nu^2). \end{aligned} \tag{2.11}$$

For given k_1, maximum four-momentum transfer is reached when the momentum of the outgoing particle is equal to $k_3 = m_\nu$, and thus $E_3 = 0$. This implies that

$$q^2_{\max} = 2\, m_\nu (k_1 - m_\nu) \approx 2 k_1 m_\nu. \tag{2.12}$$

The condition for using the effective Fermi theory for the virtual Z^0 boson exchange in figures 1(a) and (b) is $q^2 \ll M_Z^2$, which in the high-energy limit can be reformulated as

$$q^2 \approx 2 k_1 m_\nu \approx 2 E_1 m_\nu \ll M_Z^2, \qquad E_1 \ll \frac{M_Z^2}{m_\nu} \sim \frac{(10^{11}\,\text{eV})^2}{1\,\text{eV}} \sim 10^{22}\,\text{eV}, \tag{2.13}$$

where we have conservatively estimated the neutrino mass parameter to be on the order of 1 eV. (In general, one estimates the neutrino masses to be of order $(0.01 \div 0.05)$ eV, see section 1 of [48] and the discussion around equation (14.21) of [49].) The condition $E_1 \ll 10^{22}\,\text{eV} = 10^7\,\text{PeV}$ is easily fulfilled by the most energetic neutrinos seen by the IceCube collaboration [22, 23], which do not exceed $\sim$2 PeV in energy. Hence, we can safely assume Fermi theory to be valid in the entire range of incoming neutrino energies relevant for the current investigation.

2.4. 'Rest' frame of the tachyon

Let us briefly analyze the role of the 'rest frame' of the faster-than-light, incoming neutrino in the context of the tachyonic dispersion relation $E = \sqrt{k^2 - m_\nu^2}$. As is evident from a Minkowski diagram (see figure 2), the rest frame of the tachyonic 'space-like' neutrino cannot be reached via a Lorentz transformation. By contrast, for a tachyon, it is possible to transform into a frame where the *time interval* (not the space interval!) swept on the tachyonic trajectory is zero, i.e., the tachyonic particle assumes an infinite velocity. This frame of infinite velocity, in some sense, constitutes the equivalent of the rest frame; namely, the incoming particle has zero time evolution (as opposed to zero space evolution), and thus infinite velocity. According to tachyonic kinematics, it then has zero energy. For illustration, we consider the boost into a frame with energy $0 < u < 1$ (see figure 3),

$$E' = \gamma\,(E - u\,k), \qquad k' = \gamma\,(k - u\,E), \qquad E = \sqrt{k^2 - m_\nu^2}. \tag{2.14}$$

For a boost velocity $u = E/k = \sqrt{k^2 - m_\nu^2}/k < 1$, we have $E' = 0$, $k' = m$.

One might be tempted to suggest that the decay rate calculation could be simplified in the tachyonic 'rest' frame (with respect to the time, not space, i.e., $E' = 0$). However, in this

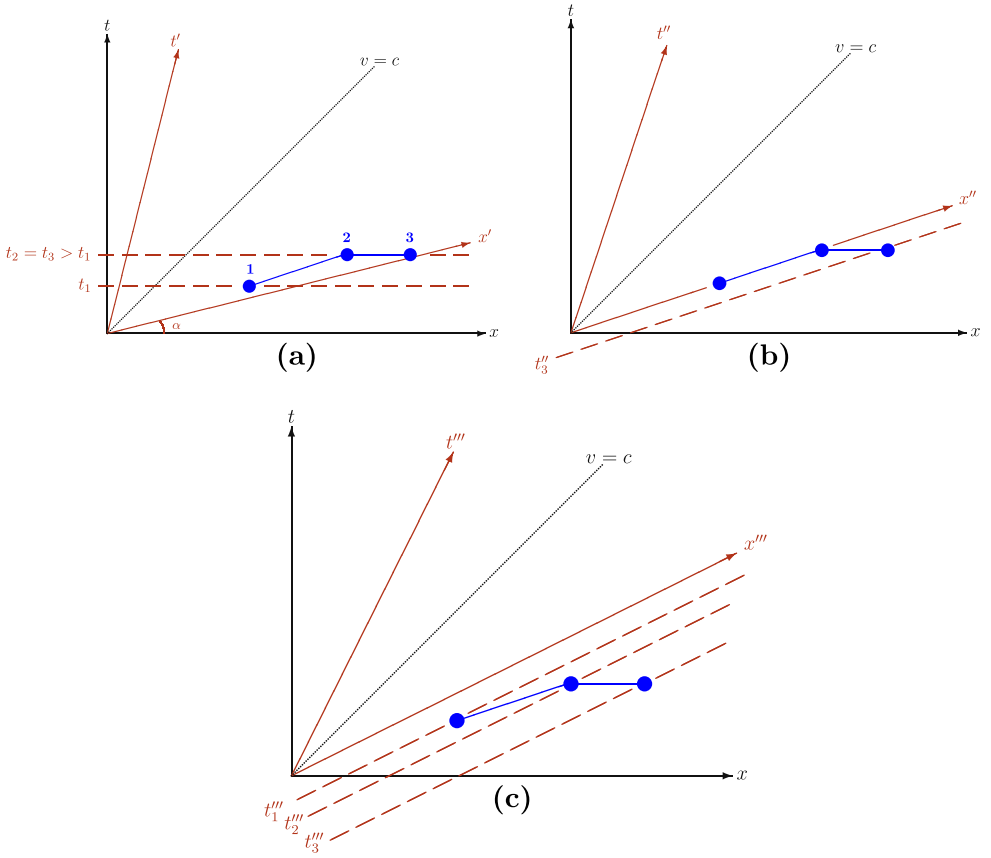

Figure 2. An incoming tachyonic neutrino follows the world line $1 \mapsto 2 \mapsto 3$, decaying into a zero-energy, infinitely fast neutrino (a). In the primed frame in (a), the time ordering of the trajectory $2 \mapsto 3$ is reversed. The initial neutrino has turned into a zero-energy decay 'product' in (b). Complete reversal of the time ordering of the decay process takes place in (c), where the moving observer (in the triple-primed frame) interprets the process as the decay of an incoming antineutrino along the trajectory $3 \mapsto 2 \mapsto 1$. Further explanations are in the text.

frame, one cannot calculate the decay rate. This is most easily seen from an energy conservation condition. The oncoming neutrino energy vanishes for infinite velocity ($E' = 0$). Hence, the oncoming particle cannot provide the energy necessary to produce an electron–positron pair.

By contrast and for comparison, for a tardyonic (subluminal) particle, the Dirac 'gap' between positive-energy and negative-energy states ensures that the energy of an oncoming, say, muon, is always bound by its rest mass m_μ from below, even under a Lorentz transformation. Hence, the muon decay from rest, with $E = m_\mu \gg 2m_e$, is kinematically possible. Because the oncoming muon is timelike, the emitted virtual W boson can still carry enough momentum transfer $q^2 > 0$ in order to produce an electron, and an electron antineutrino. This is not the case for an oncoming tachyonic neutrino, whose energy is not bound from below, and can in fact vanish. When the oncoming neutrino energy vanishes, so does the decay rate.

Alternatively, one can observe that in its own rest frame (the 'real rest frame' where the tachyon has a vanishing spatial momentum), the neutrino has the following properties,

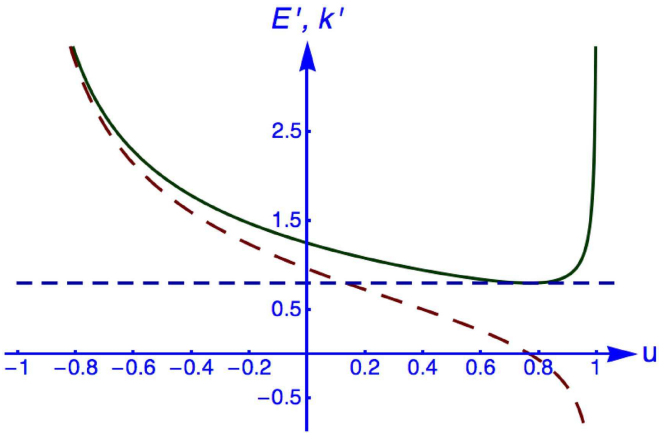

Figure 3. Lorentz-transformed momentum vector k' and transformed energy E' of a tachyonic neutrino, for boost velocities $-1 < u < 1$. In the lab frame ($u = 0$), we have $k = 1.25$ and $-m_\nu^2 = -(0.8)^2$. Under a Lorentz transformation, the modulus of the momentum vector k' indeed never gets smaller than $k' > m_\nu$ (see the solid curve). The energy E' (indicated by long dashes), however, can go to zero, and in fact changes sign at the point where the modulus of the momentum vector just becomes equal to $k' = m_\nu$ which is the point of infinite velocity. (The constant curve $k' = m_\nu$ is indicated via short dashes.) When the energy E' changes sign, the propagation direction of the neutrino changes sign, and it moves in the negative x direction as opposed to the positive x direction. From the plot (solid curve), one might think that the momentum component along the boost does not change sign, but this is not physical. From the Minkowski diagram (see figure 2), one sees that the neutrino is still moving along the positive x axis, but with the time ordering of the start and end point interchanged.

$$v_\nu = 0, \qquad k_\nu = \frac{m_\nu v_\nu}{\sqrt{v_\nu^2 - 1}} = 0, \tag{2.15}$$

but

$$E_\nu = m_\nu \Big/ \sqrt{0^2 - 1} = \sqrt{k_\nu^2 - m_\nu^2} = \sqrt{0^2 - m_\nu^2} = \mathrm{i}\, m_\nu. \tag{2.16}$$

The energy becomes imaginary in its own rest frame. According to figure 3, the rest frame of a space-like, tachyonic neutrino cannot be reached via a Lorentz transformation, consistent with the purely real (rather than complex) quantities which enter equation (2.14). A further kinematic consideration is illustrative. Namely, according to figure 3, the energy of the tachyonic particle decreases as one 'chases' it, then approaches zero and eventually flips sign at boost velocity u. For boost velocities beyond this point, the energy becomes negative, or alternatively, the time ordering of the start and end point of the trajectory of the tachyon reverses. A left-handed tachyonic neutrino, for boost velocities beyond u, would be seen as a right-handed antitachyon moving in the opposite spatial direction, for the moving observer. The spatial momentum k', as seen from figure 3, always remains in the region $k' \geqslant m_\nu$. The region with imaginary energies $E_\nu = \pm \mathrm{i} \sqrt{m_\nu^2 - \vec{k}_\nu^{\,2}}$ with $k_\nu < m_\nu$, never can be reached for an initial plane-wave tachyonic state with $k_\nu > m_\nu$, via a Lorentz transformation.

These considerations, together, afford an immediate explanation for the observation that the final result for the decay rate must necessarily vanish with the energy of the oncoming neutrino, and in fact, shall later be seen to contain the neutrino energy as a linear term. The

calculation of the decay rate of the tachyonic neutrino needs to be done in the laboratory frame (lab frame).

2.5. Particle–antiparticle transformations and tachyonic decays

A few final considerations regarding the time ordering of tachyonic world lines and the calculation of the decay rate are in order. As already emphasized, decay rates are normally calculated most easily in the rest frame of the decaying particle. For tachyons, we cannot go into the true rest frame of the decaying particle, because the frame with $k' = 0$ cannot be reached for a tachyon, as already described. In the case of a tardyonic particle, there is an energy gap of twice the rest mass between the spectrum of positive-energy (particle) versus negative-energy (anti-particle) states. This energy gap vanishes for tachyons. A tardyonic oncoming particle state cannot transform into an incoming anti-particle state, irrespective of the Lorentz frame in which the process is observed. This implies that, e.g., for the decay of an oncoming muon into a muon neutrino, electron and electron antineutrino, there is no Lorentz frame in which the same process would be observed as a time-reversed process, i.e., the annihilation of an incoming muon antineutrino and an incoming muon, into a W boson, and the eventual production of an electron and an electron antineutrino.

Furthermore, it is known that the energy of a tachyonic particle may change sign upon a Lorentz transformation (see figure 3), so that particle trajectories may become anti-particle trajectories (with the time ordering of start and end points reversed). Indeed, the fact that some particle creation and annihilation operators transform into anti-particle operator upon a Lorentz transformation, has been mentioned as an important problematic aspect of tachyonic field theories [13–21], while possible re-interpretations have recently been discussed in [6].

For a tachyonic decay of an oncoming initial tachyonic neutrino into an electron–positron pair, and an energetically lower neutrino, this means the following. The interpretation of the process may depend on the Lorentz frame in which it is observed; tachyonic trajectories have no definite time ordering. (The only ordering in the tachyonic case concerns the helicity: a left-handed particle state will transform into a right-handed anti-particle state, and vice versa.) The decay of a highly energetic oncoming neutrino ('Big Bird', see [22, 23]) into a energetically lesser one ('Tweety') via electron–positron pair production is interpreted equivalently as the annihilation of an incoming tachyonic neutrino, and an incoming tachyonic antineutrino, in specific Lorentz frames (see figure 2(b)). In other Lorentz frames, it is even reinterpreted as the decay of an incoming highly energetic antineutrino, into a less energetic antineutrino and an electron–positron pair (see figure 2(c)).

We now consider the kinematics of the tachyonic decays displayed in figure 2 in detail. In figure 2(a), the world-line trajectories of the oncoming neutrino (joining space-time points labeled 1 and 2) and of the final zero-energy neutrino (joining space-time points labeled 2 and 3) are displayed. When 'chasing' the decaying neutrino with a Lorentz boost, transforming the x and t axes into x' and t', respectively, then from visual inspection, it is evident that the time ordering on the final decay product trajectory has reversed ($t_2 = t_3$ but $t_3' < t_2'$). The decay product has turned into an incoming antineutrino, and the Lorentz-transformed process describes neutrino–antineutrino annihilation (into an electron–positron pair, but the world lines of the decay products are not displayed in figure 2). Physical reality has to be ascribed to both interpretations [13–16]. The observation of the moving ('primed') observer is equally valid. For the lab frame, this means that unless we have a counter-propagating beam of antineutrinos, the neutrino–antineutrino annihilation process does not contribute to the discussion of the 'decay', which only converts the oncoming highly energetic neutrino into one with lesser energy.

Let us now consider figure 2(b). The incoming neutrino is chased by a 'faster' Lorentz boost. The transformed axes become x'' and t'', and the first, the decaying neutrino, now constitutes a zero-energy decay product, for the decay of an incoming antineutrino (time-ordered trajectory $3 \mapsto 2$). As the boost velocity crosses the x'' and t'' axes, the decay 'product' (from the point of view of the lab frame) has turned into an incoming, highly energetic, antineutrino, which in the triple-primed frame in figure 2(c), decays into an energetically lower antineutrino (from the point of view of the boosted frame). At the point where the x'' and t'' axes are crossed, the initial, incoming neutrino has transformed into an outgoing zero-energy neutrino or antineutrino state (the interpretation changes exactly at the point where the energy changes sign).

What do these considerations imply for the description of the tachyonic decay of a neutrino? We are working in the lab frame, and we need to calculate the process in the lab frame. Processes with incoming antineutrinos must be excluded from the integration, because they cannot contribute to the decay of an incoming neutrino. The interpretation of a process involving tachyons may depend on the Lorentz frame; for the calculation of the decay rate, only processes with incoming and outgoing positive-energy neutrino states may be considered, even if these states may transform into anti-particle states upon a Lorentz transformation. The final results are still Lorentz-invariant, as discussed below in section 5.3.

3. Lepton pair Cerenkov radiation

3.1. Interaction terms in Glashow–Weinberg–Salam theory

In order to proceed to the calculation of the decay rate of the tachyonic, incoming neutrino, we briefly compile known Lagrangians from standard electroweak theory (see also appendix A). We denote the weak coupling constant as g_w. According to chap 12 of [50], quantum electrodynamics is described by the coupling of the electron to the photon,

$$\mathcal{L}_1 = -g_w \sin\theta_{\rm W} (\bar{e}\, \gamma^\mu e)\, A_\mu, \tag{3.1}$$

where $\theta_{\rm W}$ is the Weinberg angle and e and $\bar{e}$ describe the electron–positron field operators, while A_μ is the electromagnetic field operator. Furthermore, the charged vector boson $W^\pm$ interacts with a neutrino-electron current,

$$\begin{aligned}\mathcal{L}_2 = &\left\{ -\frac{g_w}{2\sqrt{2}} [\bar{e}\, \gamma^\rho (1 - \gamma^5)\, \nu_e]\, W_\rho^+ + \text{h.c.} \right\} \\ &+ \left\{ -\frac{g_w}{2\sqrt{2}} [\bar{\nu}_\mu\, \gamma^\rho (1 - \gamma^5)\, \mu]\, W_\rho^- + \text{h.c.} \right\},\end{aligned} \tag{3.2}$$

where the addition of the Hermitian adjoint is necessary in order to include the W^+ boson. For the calculation of the muon decay, one needs the full Lagrangian given in equation (3.2), even twice, namely, once for the muon–muon-neutrino current, and a second time for the decay of the W into the electron and electron antineutrino, i.e., the same current is used in the electron and in the neutrino sector.

For the decay process of the tachyonic neutrino, one needs the coupling of the neutrino to the Z^0 boson,

$$\mathcal{L}_3 = -\frac{g_w}{4\cos\theta_{\rm W}} [\bar{\nu}\, \gamma^\mu (1 - \gamma^5)\, \nu]\, Z_\mu, \tag{3.3}$$

as well as the coupling of the left- and right-handed electron to the Z^0 boson,

$$\begin{aligned}\mathcal{L}_4 &= \frac{g_w}{4\cos\theta_{\rm W}}\,\bar{e}\,[\gamma^\mu(1-\gamma^5) - 4\sin^2(\theta_{\rm W})\,\gamma^\mu]\,e\,Z_\mu \\ &= -\frac{g_w}{2\cos\theta_{\rm W}}\,\bar{e}\,[c_{\rm V}\,\gamma^\mu - c_{\rm A}\,\gamma^\mu\,\gamma^5]\,e\,Z_\mu, \\ c_{\rm V} &= -\frac{1}{2} + 2\sin^2(\theta_{\rm W}), \qquad c_{\rm A} = -\frac{1}{2}. \end{aligned} \tag{3.4}$$

The latter form allows us to identify the vector coupling and axial-vector coupling coefficient $c_{\rm V}$ and $c_{\rm A}$. According to equation (12.237) of [50], the vacuum-expectation value v of the Higgs, the weak coupling constants g_w and g_w', and the masses of the vector gauge bosons $W^\pm$, Z^0 and A, are related by

$$\begin{aligned} &M_W = \frac{1}{2}\,v\,g_w, \quad M_Z = \frac{1}{2}\,v\,(g_w^2 + g_w'^2)^{1/2}, \\ &M_A = 0, \quad \frac{M_W}{M_Z} = \frac{g_w}{(g_w^2 + g_w'^2)^{1/2}} = \cos\theta_W \approx \frac{\sqrt{3}}{2} \approx 0.877. \end{aligned} \tag{3.5}$$

These values match the experimental observations of $M_W = 80.385(15)\,\text{GeV}/c^2$ and $M_Z = 91.1876(21)\,\text{GeV}/c^2$. The matching with Fermi's effective coupling constant is given as

$$\frac{G_{\rm F}}{\sqrt{2}} = \frac{g_w^2}{8\,M_W^2}. \tag{3.6}$$

Let us anticipate a certain consideration regarding the prefactors encountered in the calculation of invariant matrix elements, in the weak decay of the muon, and in the weak decay of a tachyonic neutrino. For the weak decay of the muon, one uses the Lagrangian (3.2), whose prefactors give a numerical factor $1/(2\sqrt{2})^2 = 1/8$. For the weak decay by LPCR, we need to use the Lagrangians (3.3) and (3.4), whose combination results in a prefactor

$$\left(-\frac{1}{4\cos\theta_{\rm W}}\right) \times \left(-\frac{1}{2\cos\theta_{\rm W}}\right) = \frac{1}{8\cos^2\theta_{\rm W}}. \tag{3.7}$$

However, the weak decay of the tachyonic neutrino is mediated by a Z boson as opposed to a W boson, which results in a factor

$$\frac{1}{8\cos^2\theta_{\rm W}}\,\frac{g_w^2}{M_Z^2} = \frac{g_w^2}{8\,(\cos\theta_{\rm W}\,M_{\rm Z})^2} = \frac{G_{\rm F}}{\sqrt{2}}, \tag{3.8}$$

which is the same prefactor that we encounter in the invariant matrix element for the weak decay of the muon.

3.2. Degrees of freedom in three-body decay

Let us analyze the degrees of freedom in the phase-space of the final state, in three-body decay of a tachyonic neutrino into a less energetic neutrino, and a light fermion–antifermion

pair. The momentum transfer is $q^2 > (2m_e)^2$ from the first fermion line. The decay rate is then obtained as an integral over the differential decay rate,

$$\mathrm{d}\Gamma = \mathrm{d}^3k_1\, \mathrm{d}^3k_2\, \mathrm{d}^3k_3\, \delta^{(4)}(p_1 + p_2 + p_3). \tag{3.9}$$

This decay rate is 9 times differential, with 4 conservation conditions. We thus have 5 effective free variables.

These can be assigned as follows: for the decay of a tachyonic neutrino via pair production, we may fix the three momentum components of the outgoing neutrino. Because both the incoming as well as the outgoing neutrino have to be on the mass shell, this fixes the four-vector $q^\mu = p_1^\mu - p_3^\mu = (q^0, \vec{q})$ completely. We can then go into the rest frame of the virtual Z^0 boson and argue that the decay must be completely symmetric there; i.e., the electron and positron should come out in directions exactly opposite of each other. This gives us two more degrees of freedom, namely, the polar and azimuthal angles of one of the outgoing fermions.

The three momenta of the outgoing neutrino and the two light fermion angles add up to the five effective degrees of freedom. So, once we have $q^\mu = (q^0, \vec{q})$, we have only two degrees of freedom left for the electron–positron pair.

3.3. Rationale of the investigation

The rationale behind the calculations reported below can be summarized as follows. We shall approach the eventual calculation of the decay rate of a tachyonic neutrino due to electron–positron pair production in two steps.

- Step 1 (Complexities in the lab frame): as already emphasized, the tachyonic calculation, in which we are eventually interested, requires us to consider amplitudes in the lab frame, as opposed to the rest frame of the decaying particle. We thus need experience with calculations in the lab frame. The calculation of the muon decay rate is in principle very well-known for the rest frame of the decaying particle. Here, we generalize the calculation to a muon decay rate calculation in the lab frame, where as we shall see, the allowed $\vec{k}_3$ momenta (in the conventions used for figure 1) are inside an ellipsoid. Lorentz invariance of the integral over the allowed outgoing momenta is explicitly shown.
- Step 2 (Decay of tachyonic, space-like particles): in the calculation of the decay rate of the tachyonic neutrino, we assume (in the spirit of figure 1) that both the incoming as well as the outgoing neutrinos are on the tachyonic mass shell, $E_1 = (\vec{k}_1^{\,2} - m_\nu^2)^{1/2}$ and $E_3 = (\vec{k}_3^{\,2} - m_\nu^2)^{1/2}$. Under these circumstances, tachyonic decay is made possible exclusively due to the mass terms in the dispersion relations; hence we cannot ignore these terms Furthermore, as we have already discussed, we need to remember that the region with $|\vec{k}_3| < m_\nu$ actually is excluded from the region of allowed tachyonic momenta. We find that the physically allowed outgoing momenta are located inside the rotationally symmetric, shallow hull of a cupola-like structure, centered about the axis of the oncoming (decaying) neutrino (which we choose to be the positive z axis). As already anticipated in section 2.5, we shall need to explicitly exclude from the calculation any processes related to neutrino–antineutrino annihilation. This necessity, in turn, makes the use of the explicit spinor solutions of the tachyonic Dirac equation [6, 9] necessary.

In the calculation, we also need to overcome the pitfall connected with the time ordering of the tachyonic trajectories, anticipated in section 2.5.

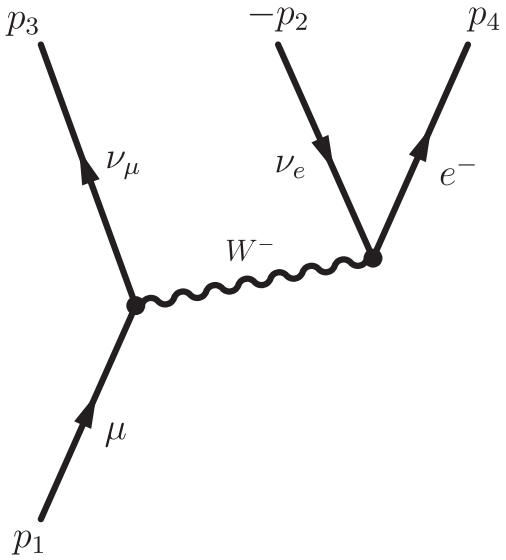

Figure 4. Conventions for muon decay.

3.4. Step 1: Integrating the muon decay width in the lab frame

We shall consider the weak decay of the muon, in the conventions of figure 4. The interaction terms from the electroweak standard model is used according to equation (3.2). For momentum transfers $q^2 \ll M_W^2$, the effective four-fermion Lagrangian thus is

$$\begin{aligned}\mathcal{L} &= \frac{g_w^2}{8\,M_W^2}(\overline{\nu}_\mu\,\gamma_\lambda\,(1-\gamma^5)\,\mu)(\overline{e}\,\gamma^\lambda\,(1-\gamma^5)\nu_e)\\ &= \frac{G_\mathrm{F}}{\sqrt{2}}(\overline{\nu}_\mu\,\gamma_\lambda\,(1-\gamma^5)\,\mu)(\overline{e}\,\gamma^\lambda\,(1-\gamma^5)\nu_e),\end{aligned} \tag{3.10}$$

where we use the matching (3.6). The Lorentz-invariant matrix element thus is (within the conventions of figure 4)

$$\mathcal{M} = \frac{G_\mathrm{F}}{\sqrt{2}}(\overline{u}(p_3)\,\gamma_\lambda\,(1-\gamma^5)u(p_1))(\overline{u}(p_4)\,\gamma^\lambda\,(1-\gamma^5)v(p_2)). \tag{3.11}$$

Summing over the final spin states and averaging over the spin projections of the initial state leads to

$$\begin{aligned}\frac{1}{2}\sum_{\text{spins}}|\mathcal{M}|^2 &= \frac{G_\mathrm{F}^2}{4}\,\mathrm{Tr}[\not{p}_3\,\gamma_\lambda\,(1-\gamma^5)(\not{p}_1+m_\mu)\gamma_\nu\,(1-\gamma^5)]\\ &\quad\times\,\mathrm{Tr}[\not{p}_2\,\gamma^\lambda\,(1-\gamma^5)(\not{p}_4+m_e)\gamma^\nu\,(1-\gamma^5)]\\ &= \frac{G_\mathrm{F}^2}{4}[256\,(p_1\cdot p_2)\,(p_3\cdot p_4)] = 64\,G_\mathrm{F}^2\,(p_1\cdot p_2)\,(p_3\cdot p_4).\end{aligned} \tag{3.12}$$

The procedure of integration in the rest frame of the decaying particle is discussed in equation (10.16) ff. of [12]. Furthermore, a mixed approach, where certain intermediate integrals are

carried out covariantly, and only the final stages of the calculation are carried out in the rest frame of the decaying particle, is outlined in chap 7.2.2 of [51]. In the actual evaluation, in the conventions of figure 4, we keep the outgoing neutrino momentum as our final integration variable and write the decay rate in the lab frame as follows (for the expression in the lab frame, see [52]),

$$\begin{aligned}
\Gamma &= \frac{1}{2E_1} \int \frac{\mathrm{d}^3k_3}{(2\pi)^3\,2E_3}\Bigg(\int \frac{\mathrm{d}^3k_2}{(2\pi)^3\,2E_2} \int \frac{\mathrm{d}^3k_4}{(2\pi)^3\,2E_4} (2\pi)^4\,\delta^{(4)}(p_1 - p_3 - p_2 - p_4) \\
&\quad \times \left[\frac{1}{2} \sum_{\text{spins}} |\mathcal{M}|^2\right]\Bigg) \\
&= \frac{1}{2E_1} \int \frac{\mathrm{d}^3k_3}{(2\pi)^3\,2E_3}\Bigg(\int \frac{\mathrm{d}^3k_2}{(2\pi)^3\,2E_2} \int \frac{\mathrm{d}^3k_4}{(2\pi)^3\,2E_4} \\
&\quad \times (2\pi)^4\,\delta^{(4)}(p_1 - p_3 - p_2 - p_4)[64 G_{\mathrm{F}}^2 (p_1 \cdot p_2)\,(p_3 \cdot p_4)]\Bigg) \\
&= \frac{2\,G_{\mathrm{F}}^2}{\pi^5\,(2E_1)} \int \frac{\mathrm{d}^3k_3}{2E_3}\Bigg(\int \frac{\mathrm{d}^3k_2}{2E_2} \int \frac{\mathrm{d}^3k_4}{2E_4} (2\pi)^4\,\delta^{(4)}(p_1 - p_3 - p_2 - p_4) \\
&\quad \times (p_1^\lambda \cdot p_{2\lambda})\,(p_{3\rho} \cdot p_4^\rho)\Bigg) \\
&= \frac{2\,G_{\mathrm{F}}^2}{\pi^5\,(2E_1)} \int \frac{\mathrm{d}^3p_3}{2E_3} (p_1^\lambda p_3^\rho\, J_{\lambda\rho}(p_1 - p_3)) = \frac{G_{\mathrm{F}}^2}{12\,\pi^4\,(2E_1)} \\
&\quad \times \int \frac{\mathrm{d}^3p_3}{2E_3}\, p_1^\lambda p_3^\rho (g_{\lambda\rho}\, q^2 + 2\, q_\lambda\, q_\rho) \\
&= \frac{G_{\mathrm{F}}^2}{12\,\pi^4\,(2E_1)} \int \frac{\mathrm{d}^3k_3}{2E_3} (p_1 \cdot p_3\, q^2 + 2\,(p_1 \cdot q)\,(p_3 \cdot q)).
\end{aligned} \tag{3.13}$$

We have used the following result, derived in equation (B.1), which is obtained for two outgoing particles with labels 2 and 4 which are on the electronic mass shell $p_2^2 = p_4^2 = m_e^2$,

$$\begin{aligned}
J_{\lambda\rho}(q) &= \int \frac{\mathrm{d}^3k_2}{2E_2} \int \frac{\mathrm{d}^3k_4}{2E_4} \delta^{(4)}(q - p_2 - p_4)(p_{2\lambda}\, p_{4\rho}) \\
&= \sqrt{1 - \frac{4\,m_e^2}{q^2}} \left[g_{\lambda\rho}\, \frac{\pi}{24}(q^2 - 4m_e^2) + q_\lambda\, q_\rho\, \frac{\pi}{12}\left(1 + \frac{2m_e^2}{q^2}\right)\right] \\
&\approx \frac{\pi}{24}\, g_{\lambda\rho}\, q^2 + \frac{\pi}{12}\, q_\lambda\, q_\rho, \qquad m_e \to 0.
\end{aligned} \tag{3.14}$$

By symmetry, we have $J_{\lambda\rho}(q) = J_{\lambda\rho}(q)$. We have carried out the p_2 and p_4 integrals covariantly. Then, for the remaining integral over p_3, we need the appropriate integration limits. We thus need to integrate

$$\Gamma = \frac{G_{\mathrm{F}}^2}{12\,\pi^4\,(2E_1)} \int \frac{\mathrm{d}^3k_3}{2E_3} (p_1 \cdot p_3\, q^2 + 2\,(p_1 \cdot q)\,(p_3 \cdot q)), \tag{3.15}$$

assuming an incoming muon with energy E_1 in the positive z direction, with the incoming p_1 on the muon mass shell, $p_1^2 = m_\mu^2$. The final p_3 describes the muon neutrino, so that within

our approximations $(p_3)^2 \approx 0$. The domain of the d^3p_3 integration in equation (3.15) contains all four-momenta p_3 for which $q^2 = (p_1 - p_2)^2 > 0$.

In the rest frame of the decaying muon, the integration domain would consist of a sphere composed of vectors $p_3 = (|\vec{k}_3|, \vec{k}_3)$, with $p_1 = (E_1, \vec{0})$ and $|\vec{k}_3| \leqslant m_\nu/2$. By contrast, in the lab fame, we consider a muon moving up the z axis, with energy E_1 and wave vector $\vec{k}_1$, and an outgoing muon neutrino with energy E_3 and wave vector $\vec{k}_3$,

$$\vec{k}_1 = k_1\,\hat{e}_z, \;\; E_1 = \sqrt{k_1^2 + m_\mu^2}, \;\; \vec{k}_3 = k_\rho\,\hat{e}_\rho + k_z\hat{e}_z, \;\; E_3 = |\vec{k}_3| = \sqrt{k_\rho^2 + k_z^2}. \tag{3.16}$$

The momentum transfer reads as follows,

$$q^2 = 2k_1\,k_z + m_\mu^2 - 2\sqrt{k_\rho^2 + k_z^2}\,\sqrt{k_1^2 + m_\mu^2}. \tag{3.17}$$

The allowed vectors $\vec{k}_3$ are located inside a rotationally symmetric ellipsoid (see figure 5), which is centered at the point $(0, 0, k_{z0})$ on the z axis. Let us denote by a the half axis of the ellipsoid in the radial direction ('away' from the z axis) and by b the half axis of the ellipsoid in the z direction (see figure 5). These half axes are given as follows,

$$a = \frac{m_\mu}{2}, \qquad b = \frac{1}{2}\,\sqrt{k_1^2 + m_\mu^2}, \qquad k_{z0} = \frac{k_1}{2}. \tag{3.18}$$

For the integration of the final phase-space in the expression (3.15), we need to calculate

$$\Gamma = \frac{G_F^2}{12\,\pi^4\,(2E_1)} \int_{q^2=(p_1-p_3)^2>0} \frac{d^3p_3}{2E_3}(p_1\cdot p_3\,q^2 + 2\,(p_1\cdot q)\,(p_3\cdot q)). \tag{3.19}$$

One uses the following parameterization ($k_x \equiv k_{3x}$, $k_y \equiv k_{3y}$, and $k_z \equiv k_{3z}$),

$$k_x = a\,\xi\,\sin\theta\cos\varphi, \;\; k_y = a\,\xi\,\sin\theta\,\sin\varphi, \;\; k_z = k_{z0} + b\,\xi\cos\theta. \tag{3.20}$$

The Jacobian is

$$d^3k_3 = \left| \det\begin{pmatrix} \frac{\partial k_x}{\partial\xi} & \frac{\partial k_x}{\partial\theta} & \frac{\partial k_x}{\partial\varphi} \\ \frac{\partial k_y}{\partial\xi} & \frac{\partial k_y}{\partial\theta} & \frac{\partial k_y}{\partial\varphi} \\ \frac{\partial k_z}{\partial\xi} & \frac{\partial k_z}{\partial\theta} & \frac{\partial k_z}{\partial\varphi} \end{pmatrix} \right| = a^2\,b\,\xi\,\sin\theta. \tag{3.21}$$

Then, with $u = \cos\theta$ and $k_1 = \chi m_\mu$, one has after the trivial integration over φ,

$$\Gamma = \frac{G_F^2 m_\mu^6}{12\,\pi^3\,(2E_1)} \int_0^1 d\xi \int_{-1}^1 du\, \frac{\xi^2\,\sqrt{1+\chi^2}}{8\,\sqrt{\xi(\xi(1+u^2\,\chi^2) + 2u\sqrt{1+\chi^2}\,\chi) + \chi^2}}$$
$$\times\,[(4\xi\,u\chi(\chi^2+1) + (4\chi^2+3)\,\sqrt{\chi^2+1})\,\sqrt{\xi(\xi(1+u^2\,\chi^2) + 2u\sqrt{1+\chi^2}\,\chi) + \chi^2}$$
$$-\,\xi\,u\,\sqrt{\chi^2+1}\,(8\chi^2+7)\,\chi - 2\xi^2(\chi^2+1)\,(2u^2\chi^2+1) - 4\chi^2 - 5\chi^2]. \tag{3.22}$$

After a somewhat tedious u integration, the result can be written in terms of the variable

$$|\xi\,\sqrt{1+\chi^2} - \chi| = \begin{cases} \chi - \xi\,\sqrt{1+\chi^2} & 0 < \xi < \frac{\chi}{\sqrt{1+\chi^2}} \\ \xi\,\sqrt{1+\chi^2} - \chi & \frac{\chi}{\sqrt{1+\chi^2}} < \xi < 1 \end{cases}.$$

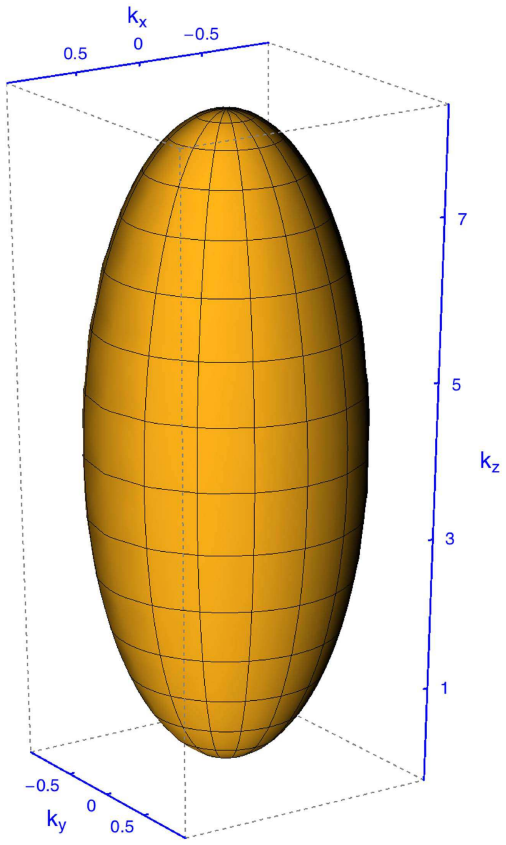

Figure 5. A muon with wave vector $k_1 = 8$ and mass $m_\mu = 2$ is incoming along the positive z direction. The electron mass as well as the neutrino masses are assumed to be negligible, and the threshold condition for weak decay into a muon neutrino, electron and electron antineutrino therefore simplifies to $q^2 = (p_1 - p_3)^2 > 0$. We investigate the boundaries of the volume of allowed k_3 vectors, with Cartesian components $k_x = k_{3x}$, $k_y = k_{3y}$, and $k_z = k_{3z}$. The z components of the allowed k_3 vectors range from $k_{3,\min} = -0.1231$ to $k_{3,\max} = 8.1231$. The geometry of allowed k_3 vectors is that of an ellipsoid, rotationally symmetric about the z axis, with parameters $a = 1$ and $b = 4.1231$ as given in equation (3.18).

The decay rate is naturally written as $\Gamma = \Gamma_1 + \Gamma_2$, where the integration domains are such that $|\xi\sqrt{1+\chi^2} - \chi|$ assumes either of the values given in equation (3.23). Here,

$$\Gamma_1 = \frac{G_F^2 m_\mu^6}{12\,\pi^3\,(2E_1)} \int_0^{\chi/\sqrt{1+\chi^2}} \frac{\mathrm{d}\xi}{8\chi}\xi\left(\sqrt{1+\chi^2}\,\ln\left(\frac{1+\xi}{1-\xi}\right)\right.$$
$$\left. - 2\xi(1+\chi^2)(\chi(4\chi\,(\sqrt{1+\chi^2} - \chi) - 3) + \sqrt{1+\chi^2})\right), \qquad (3.23a)$$

$$\Gamma_2 = \frac{G_F^2 m_\mu^6}{12\,\pi^3\,(2E_1)} \int_{\chi/\sqrt{1+\chi^2}}^1 \frac{\mathrm{d}\xi}{8\chi}\xi\left(\sqrt{1+\chi^2}\,\ln\left(\frac{1+\sqrt{1+\chi^2}}{1-\sqrt{1+\chi^2}}\right)\right.$$
$$\left. + 2\,\chi(2(1-\xi^2)\,\chi^2 - 2\xi^2 + 3\xi - 1)(1+\chi^2)\right). \qquad (3.23b)$$

The two contributions evaluate to the expressions,

$$\Gamma_1 = \frac{G_{\rm F}^2 m_\mu^6}{12\,\pi^3\,(2E_1)} \times \frac{2\chi(3+4\chi^2)\left(\sqrt{1+\chi^2}+2\chi^2(\chi-\sqrt{1+\chi^2})-3\ln\left(\frac{\sqrt{1+\chi^2}+\chi}{\sqrt{1+\chi^2}-\chi}\right)\right)}{48\,\chi\,\sqrt{1+\chi^2}}, \tag{3.24a}$$

$$\Gamma_2 = \frac{G_{\rm F}^2 m_\mu^6}{12\,\pi^3\,(2E_1)} \times \left[\frac{1}{8} - \frac{2\chi(3+4\chi^2)\left(\sqrt{1+\chi^2}+2\chi^2(\chi-\sqrt{1+\chi^2})-3\ln\left(\frac{\sqrt{1+\chi^2}+\chi}{\sqrt{1+\chi^2}-\chi}\right)\right)}{48\,\chi\,\sqrt{1+\chi^2}}\right], \tag{3.24b}$$

so that

$$\Gamma = \Gamma_1 + \Gamma_2 = \frac{G_{\rm F}^2 m_\mu^6}{12\,\pi^3\,(2E_1)} \times \frac{1}{8} = \frac{G_{\rm F}^2 m_\mu^5}{192\,\pi^3}\,\frac{m_\mu}{E_1}. \tag{3.25}$$

This is the expected result for the muon decay width, with the $1/E_1$ prefactor already included, which is here obtained directly by an explicit integration in the lab frame.

We have also verified [25] the results of Cohen and Glashow for superluminal neutrino decay, based on the noncovariant dispersion relation used in [31], via an independent calculation in the lab frame, as envisaged in [33]. The treatment described in [31] is based on a Lorentz-violating dispersion relation $E = |\vec{k}|v_\nu$ with $v_\nu > 1$, which constitutes a fundamentally different theoretical model as compared to the Lorentz-invariant tachyonic treatment presented here. In addition to the decay rate, we shall also consider the energy loss rate of an incoming neutrino beam in the lab frame, due to LPCR and NPCR. A remark is in order: the calculation of the energy loss per time of an incoming muon beam, to complement a corresponding calculation for the tachyonic neutrino beam, is not applicable, because the end product of the decay is not a less energetic muon, but the muon disappears from the beam altogether (see figure 4).

3.5. Step 2: Tachyonic neutrino decay (covariant dispersion relation)

We calculate the decay width of the incoming tachyonic neutrino, in the lab frame, employing a relativistically covariant (tachyonic) dispersion relation, with both incoming as well as outgoing neutrinos on the tachyonic mass shell ($E_1 = (\vec{k}_1^{\,2} - m_\nu^2)^{1/2}$, and $E_3 = (\vec{k}_1^{\,2} - m_\nu^2)^{1/2}$, in the conventions of figure 1). In the lab frame, in full accordance with [52], the decay rate simply is

$$\Gamma = \frac{1}{2E_1}\int \frac{{\rm d}^3p_3}{(2\pi)^3\,2E_3}\left(\int \frac{{\rm d}^3p_2}{(2\pi)^3\,2E_2}\int \frac{{\rm d}^3p_4}{(2\pi)^3\,2E_4} \times (2\pi)^4\,\delta^{(4)}(p_1-p_3-p_2-p_4)\left[\widetilde{\sum}_{\rm spins}|\mathcal{M}|^2\right]\right). \tag{3.26}$$

Here, $\widetilde{\sum}_{\text{spins}}$ refers to the specific way in which the average over the oncoming helicity states, and the outgoing helicities, needs to be carried out for tachyons. As explained in section 2.4, we cannot reach the rest frame of the decaying particle by a Lorentz transformation, in the case of a tachyonic neutrino. Furthermore, as outlined in section 2.3, a calculation with just the Fermi effective coupling constant actually is sufficient for the tachyonic case. For the relevant interaction terms, we use the same expression as in section 3.5. We recall the coupling of the decaying neutrino to the Z^0 boson according to equation (3.3),

$$\mathcal{L}_3 = -\frac{g}{4\cos\theta_{\text{W}}}\,\bar{\nu}\,\gamma^\lambda\,(1-\gamma^5)\,\nu\,Z_\lambda. \tag{3.27}$$

For the coupling of the electron to the Z boson, we have according to equation (3.4),

$$\mathcal{L}_4 = -\frac{g_w}{2\cos\theta_{\text{W}}}\,\bar{e}\,[c_{\text{V}}\,\gamma^\lambda - c_{\text{A}}\,\gamma^\lambda\,\gamma^5]\,e\,Z_\lambda, \qquad c_{\text{V}} \approx 0, \qquad c_{\text{A}} = -\frac{1}{2}. \tag{3.28}$$

In view of the compensation mechanism given by equation (3.8), the effective four-fermion Lagrangian thus is given by

$$\mathcal{L} = \frac{G_{\text{F}}}{\sqrt{2}}\{\bar{\nu}\,\gamma^\lambda\,(1-\gamma^5)\,\nu\}\,\{\bar{e}[c_{\text{V}}\,\gamma^\rho - c_{\text{A}}\,\gamma^\lambda\,\gamma^5]\,e\}. \tag{3.29}$$

The matrix element of the fundamental spinor solutions reads as follows,

$$\mathcal{M} = \frac{G_{\text{F}}}{\sqrt{2}}[\bar{u}^{\mathcal{T}}(p_3)\,\gamma_\lambda\,(1-\gamma^5)\,u^{\mathcal{T}}(p_1)][\bar{u}(p_4)(c_{\text{V}}\gamma^\lambda - c_{\text{A}}\,\gamma^\lambda\,\gamma^5)\,v(p_2)]. \tag{3.30}$$

Here, the $u^{\mathcal{T}}(p_1)$, and $u^{\mathcal{T}}(p_3)$, constitute Dirac spinor solutions of the tachyonic Dirac equation. In the helicity basis [9, 53], denoted by a subscript $\sigma = \pm$, the tachyonic particle and antiparticle spinors are

$$u_+^{\mathcal{T}}(\vec{k}) = \begin{pmatrix} \sqrt{|\vec{k}| + m}\;a_+(\vec{k}) \\ \sqrt{|\vec{k}| - m}\;a_+(\vec{k}) \end{pmatrix}, \qquad u_-^{\mathcal{T}}(\vec{k}) = \begin{pmatrix} \sqrt{|\vec{k}| - m}\;a_-(\vec{k}) \\ -\sqrt{|\vec{k}| + m}\;a_-(\vec{k}) \end{pmatrix}, \tag{3.31a}$$

$$v_+^{\mathcal{T}}(\vec{k}) = \begin{pmatrix} -\sqrt{|\vec{k}| - m}\;a_+(\vec{k}) \\ -\sqrt{|\vec{k}| + m}\;a_+(\vec{k}) \end{pmatrix}, \qquad v_-^{\mathcal{T}}(\vec{k}) = \begin{pmatrix} -\sqrt{|\vec{k}| + m}\;a_-(\vec{k}) \\ \sqrt{|\vec{k}| - m}\;a_-(\vec{k}) \end{pmatrix}, \tag{3.31b}$$

where the $a_\sigma(\vec{k})$ are the fundamental helicity spinors (see p 87 of [50]).

The properties of the tachyonic bispinor solutions differ somewhat from those of the 'normal' tardyonic bispinors. The well-known sum formula for the tardyonic states is (σ denotes the spin orientation)

$$\sum_\sigma u_\sigma(p) \otimes \bar{u}_\sigma(p) = \not{p} + m_e. \tag{3.32}$$

For the tachyonic spin sums, one has the following sum rule for the positive-energy spinors,

$$\sum_\sigma (-\sigma)\,u_\sigma^{\mathcal{T}}(p) \otimes \bar{u}_\sigma^{\mathcal{T}}(p)\,\gamma^5 = \sum_\sigma (-\vec{\Sigma}\cdot\hat{p})\,u_\sigma^{\mathcal{T}}(p) \otimes \bar{u}^{\mathcal{T}}(p)\,\gamma^5 = \not{p} - \gamma^5\,m, \tag{3.33}$$

where we use $p = (E, \vec{p})$ as the convention for the four-momentum and $\hat{p} = \vec{p}/|\vec{p}|$ is the unit vector in the $\vec{p}$ direction. Upon promotion to a four-vector, we have $\hat{p}^\mu = (0, \hat{p})$. The sum rule can thus be reformulated as

$$\sum_\sigma u_\sigma^{\mathcal{T}}(p) \otimes \bar{u}_\sigma^{\mathcal{T}}(p) = (-\vec{\Sigma}\cdot\hat{p})\,(\not{p} - \gamma^5\, m_\nu)\,\gamma^5 = -\gamma^5\,\gamma^0\,\gamma^i\,\hat{p}^i\,(\not{p} - \gamma^5\, m_\nu)\,\gamma^5$$
$$= -\not{\tau}\,\gamma^5\,\gamma^i\,\hat{p}_i\,(\not{p} - \gamma^5\, m_\nu)\,\gamma^5 = -\not{\tau}\,\gamma^5\,\not{\hat{p}}\,(\not{p} - \gamma^5\, m_\nu)\,\gamma^5, \tag{3.34}$$

where $\tau = (1, 0, 0, 0)$ is a time-like unit vector. In [6, 9], it has been established that a consistent formulation of the tachyonic propagator is achieved when we postulate that the right-handed neutrino states, and the left-handed antineutrino states, acquire a negative Fock-space norm after quantization of the tachyonic spin-1/2 field. Hence, in order to consider the decay process of an oncoming, left-handed, positive-energy neutrino, we should consider the projection onto negative-helicity states,

$$\frac{1}{2}(1 - \vec{\Sigma}\cdot\hat{p})\sum_\sigma u_\sigma^{\mathcal{T}}(p) \otimes \bar{u}_\sigma^{\mathcal{T}}(p) = u_{\sigma=-1}(p) \otimes \bar{u}_{\sigma=-1}(p)$$
$$= \frac{1}{2}(1 - \not{\tau}\,\gamma^5\,\not{\hat{p}})\,(\not{p} - \gamma^5\, m_\nu)\,\gamma^5. \tag{3.35}$$

The squared and spin-summed matrix element is

$$\sum_{\text{spins}}\!\!\!\!\!\!\sim\ |\mathcal{M}|^2 = \frac{G_{\text{F}}^2}{2}\,\text{Tr}\Bigg[\frac{1}{2}(1 - \not{\tau}\,\gamma^5\not{p}_3)\,(\not{p}_3 - \gamma^5\, m_\nu)\,\gamma^5\,\gamma_\lambda\,(1 - \gamma^5)$$
$$\times\,\frac{1}{2}(1 - \not{\tau}\,\gamma^5\,\not{p}_1)\,(\not{p}_1 - \gamma^5\, m_\nu)\,\gamma^5\,\gamma_\nu\,(1 - \gamma^5)\Bigg]$$
$$\times\,\text{Tr}[(\not{p}_4 + m_e)(c_{\text{V}}\gamma^\lambda - c_{\text{A}}\,\gamma^\lambda\,\gamma^5)\,(\not{p}_2 + m_e)(c_{\text{V}}\gamma^\rho - c_{\text{A}}\,\gamma^\rho\,\gamma^5)]$$
$$= \frac{G_{\text{F}}^2}{2}\,\mathcal{S}(p_1, p_2, p_3, p_4), \tag{3.36}$$

with $c_{\text{V}} \approx 0$, $c_{\text{A}} \approx -1/2$ (the last step implicitly defines the expression $\mathcal{S}$). Here, the meaning of the notation $\sum\!\!\!\!\!\!\sim_{\text{spins}}$ becomes clear: we have summed over the spins of the outgoing electron–positron pair, while only one specific helicity is taken into account for the oncoming (decaying) neutrino.

The Dirac γ traces in equation (3.36) give rise to a rather lengthy expression, which can be simplified somewhat because incoming and outgoing particles are on their respective mass shells, $p_2^2 = p_4^2 = m_e^2$, while on the tachyonic mass shell, we have $p_1^2 = p_3^2 = -m_\nu^2$. Some other scalar products vanish, e.g., the scalar product of the time-like unit vector τ and the space-like unit vector, which is $\tau\cdot\hat{p} = 0$.

The result of the Dirac γ traces from equation (3.36) can then be inserted into equation (3.26), and the d^3p_2 and d^3p_4 integrals can be carried out using the following formulas, which we recall from appendix B (see equation (B.1)),

$$I(q) = \int\frac{\text{d}^3p_2}{2E_2}\int\frac{\text{d}^3p_4}{2E_4}\,\delta^{(4)}(q - p_2 - p_4) = \frac{\pi}{2}\,\sqrt{1 - \frac{4\,m_e^2}{q^2}}\,, \tag{3.37}$$

$$J_{\lambda\rho}(q) = \int\frac{\text{d}^3p_2}{2E_2}\int\frac{\text{d}^3p_4}{2E_4}\,\delta^{(4)}(q - p_2 - p_4)(p_{2\lambda}\,p_{4\rho})$$
$$= \sqrt{1 - \frac{4\,m_e^2}{q^2}}\left[g_{\lambda\rho}\,\frac{\pi}{24}(q^2 - 4m_e^2) + q_\lambda\,q_\rho\,\frac{\pi}{12}\left(1 + \frac{2m_e^2}{q^2}\right)\right], \tag{3.38}$$

$$K(q) = \int \frac{\mathrm{d}^3 p_2}{2E_2} \int \frac{\mathrm{d}^3 p_4}{2E_4} \delta^{(4)}(q - p_2 - p_4)(p_2 \cdot p_4) = \frac{\pi}{4} \sqrt{1 - \frac{4\,m_e^2}{q^2}}\,(q^2 - 2m_e^2). \tag{3.39}$$

After the $\mathrm{d}^3 p_2$ and $\mathrm{d}^3 p_4$ integrations, we are left with an expression of the form

$$\Gamma = \frac{G_\mathrm{F}^2}{2} \frac{1}{(2\pi)^5} \int_{q^2 > 4m_e^2} \frac{\mathrm{d}^3 p_3}{2E_3}\, \mathcal{F}(p_1, p_3), \tag{3.40}$$

where

$$\mathcal{F}(p_1, p_3) = \int \frac{\mathrm{d}^3 p_2}{2E_2} \int \frac{\mathrm{d}^3 p_4}{2E_4} \delta^{(4)}(p_1 - p_2 - p_3 - p_4)\, \mathcal{S}(p_1, p_2, p_3, p_4). \tag{3.41}$$

Both the expressions for $\mathcal{S}(p_1, p_2, p_3, p_4)$ as well as $\mathcal{F}(p_1, p_3)$ are too lengthy to be displayed in the context of the current paper. However, approximate formulas can be given, e.g., when the incoming energy E_1 is near threshold.

In order to obtain a better intuitive picture for the domain of allowed p_3 four-vectors, we have to analyze the tachyonic kinematics in some more detail. We calculate in the lab frame and assume that the oncoming neutrino has the energy-momentum four-vector

$$\begin{aligned} p_1^\mu &= (E_1,\, 0,\, 0,\, k_1), \quad E_1 \geqslant (E_1)_\mathrm{th} = 2\frac{m_e}{m_\nu} \sqrt{m_e^2 + m_\nu^2}, \\ k_1 &\geqslant (k_1)_\mathrm{th} = 2\frac{m_e^2}{m_\nu} + m_\nu, \quad E_1^2 - k_1^2 = -m_\nu^2 \end{aligned} \tag{3.42}$$

(see equations (2.3) and (2.4)). The final-state four-vector is conveniently parameterized as

$$p_3^\mu = (E_3,\, k_3 \sin\theta \cos\varphi,\, k_3 \sin\theta \sin\varphi,\, k_3 \cos\theta), \qquad k_3 > m_\nu. \qquad E_3^2 - k_3^2 = -m_\nu^2. \tag{3.43}$$

The condition $k_3 > m_\nu$ is naturally imposed for tachyonic kinematics (see figure 3). The squared four-momentum transfer then reads as

$$\begin{aligned} q^2 &= 2(\sqrt{E_1^2 + m_\nu^2}\sqrt{E_3^2 + m_\nu^2}\cos\theta - E_1 E_3 - m_\nu^2) \\ &= 2(k_1 k_3 \cos\theta - \sqrt{k_1^2 - m_\nu^2}\,\sqrt{k_3^2 - m_\nu^2} - m_\nu^2), \end{aligned} \tag{3.44}$$

where it is convenient to define $u = \cos\theta$. One may solve for the threshold angle $\cos\theta_\mathrm{th}$,

$$q^2 = 4m_e^2 \quad \Rightarrow \quad u = \cos\theta = u_\mathrm{th} = \cos\theta_\mathrm{th} = \frac{E_1 E_3 + 2m_e^2 + m_\nu^2}{\sqrt{E_1^2 + m_\nu^2}\sqrt{E_2^2 + m_\nu^2}}. \tag{3.45}$$

For given E_1 and E_3, all angles θ with $\cos\theta > \cos\theta_\mathrm{th}$, i.e., for $\theta < \theta_\mathrm{th}$, are permissible. Conversely, setting $\cos\theta_\mathrm{th} = 1$ and $E_3 = 0$, one may solve for E_1 and rederive the threshold condition (2.3). All of this implies that the domain of permissible $\vec{k}_3$ vectors, near threshold, is centered about the z axis and forms a 'cupola' of inner radius m_ν (see figure 6). Within the kinematically allowed region, the tachyonic momentum transfer q^2 is plotted in figure 7.

For given E_1, the widest opening angle $\theta = \theta_\mathrm{th}$ is reached when E_3 becomes zero. One finds

$$\cos\theta_\mathrm{th}|_{E_3=0} = \frac{2m_e^2 + m_\nu^2}{m_\nu \sqrt{E_1^2 + m_\nu^2}} \approx \left(\frac{2m_e^2}{m_\nu} + m_\nu\right) E_1^{-1} = \frac{k_\mathrm{th}}{E_1}, \tag{3.46}$$

where the latter form is valid in the high-energy limit. Here, $k_\mathrm{th} = \frac{2m_e^2}{m_\nu} + m_\nu$ is the threshold momentum. It means that the produced pairs will be emitted in a very narrow cone, centered in the forward direction with respect to the decaying neutrino.

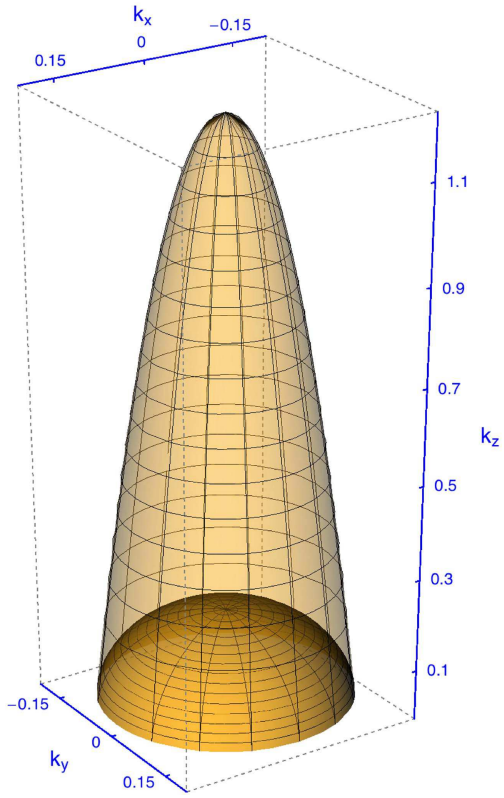

Figure 6. A tachyonic neutrino with wave vector $k_1 = 122$ and mass $-m_\nu^2 = -(0.2)^2$ is incoming along the positive z direction. The electron mass is set equal to unity, $m_e = 1$. The threshold condition therefore reads as $q^2 = (p_1 - p_3)^2 \geqslant 4$. The boundaries of the volume of allowed k_3 vectors, with Cartesian components $k_x = k_{3x}$, $k_y = k_{3y}$, and $k_z = k_{3z}$, are mainly concentrated in a narrow, rotationally symmetric cone about the z axis. Final states with $|\vec{k}_3| < m_\nu$ correspond to evanescent outgoing waves, lead to a complex-valued momentum transfer, and have to be excluded.

Maximum squared momentum transfer is reached at $E_3 = 0$ and $\theta = 0$,

$$q^2 = q^2_{\max} = 2\,m_\nu(\sqrt{E_1^2 + m_\nu^2} - m_\nu) = 2\,m_\nu(k_1 - m_\nu), \tag{3.47}$$

confirming equation (2.12). Maximum outgoing energy E_3 is reached for minimum momentum transfer $q^2 = q^2_{\min} = 4m_e^2$, with the final-state neutrino propagating into the positive z direction. Its energy is

$$(E_3)_{\max} = E_1\left(2\,\frac{m_e^2}{m_\nu^2} + 1\right) - \frac{2m_e\,\sqrt{E_1^2 + m_\nu^2}\,\sqrt{m_e^2 + m_\nu^2}}{m_\nu^2} \approx \frac{E_1\,m_\nu^2}{4m_e^2}, \tag{3.48}$$

where the latter form is valid in the limit of large E_1. This corresponds to the maximum allowed k_3,

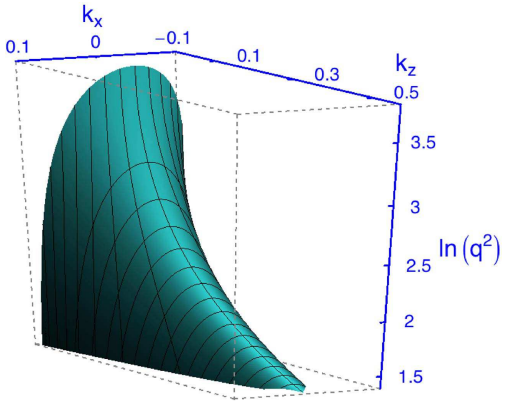

Figure 7. Plot of the tachyonic momentum transfer q^2 in the kinematically allowed region, for an oncoming neutrino (along the positive z direction) with parameters $k_1 = 223$, $m_\nu = 0.1$, and $m_e = 1$. The lines on the surface describe constant angle θ. and lines of constant $|\vec{k}_3|$. We set $k_y = 0$, which would otherwise correspond to an azimuth angle $\varphi = 0$ for the outgoing neutrino momentum $\vec{k}_3$. The vector modulus $k_3 = |\vec{k}_3|$ varies from its minimum tachyonic value of $(k_3)_{\min} = m_\nu = 0.1$ to the maximum value $(k_3)_{\max}$ given in equation (3.49). For maximum k_3, q^2 assumes the threshold value $q^2 = 4m_e^2 = 4$. The maximum q^2 is reached at the minimum value for k_3, and for collinear geometry, $\theta_3 = 0$, and reads as $(q^2)_{\max} = 44.58$ (see equation (3.47)).

$$(k_3)_{\max} = \frac{k_1(2m_e^2 + m_\nu^2) - 2m_e\sqrt{k_1^2 - m_\nu^2}\,\sqrt{m_e^2 + m_\nu^2}}{m_\nu^2} \approx \frac{k_1\, m_\nu^2}{4m_e^2}, \tag{3.49}$$

where, again, the latter form is valid in high-energy limit $k_1 \to \infty$. A plot of the physically relevant range for q^2 is given in figure 7.

Because of azimuthal symmetry, it is easily possible to find a convenient parameterization of the regime of allowed $\vec{k}_3$ in spherical coordinates (using the parameterization given in equation (3.43)). We may finally express the integrand $\mathcal{F}$ from equation (3.41) in terms of the initial and final energies E_1 and E_3 of the decay process, and of the scattering angle θ (with $u = \cos\theta$). The decay rate given by equation (3.40) can thus be written as follows,

$$\begin{aligned}\Gamma &= \frac{G_F^2}{2}\frac{1}{(2\pi)^5}\int_0^{2\pi} \mathrm{d}\varphi \int_{(k_3)_{\min}}^{(k_3)_{\max}} \frac{\mathrm{d}k_3\, k_3^2}{2E_3} \int_{u_{\rm th}}^{1} \mathrm{d}u\, \mathcal{F}(E_1, E_3, u) \\ &= \frac{G_F^2}{4}\frac{1}{(2\pi)^4}\int_{(E_3)_{\min}}^{(E_3)_{\max}} \mathrm{d}E_3\, \sqrt{E_3^2 + m_\nu^2} \int_{u_{\rm th}}^{1} \mathrm{d}u\, \mathcal{F}(E_1, E_3, u).\end{aligned} \tag{3.50}$$

Here, $(k_3)_{\min} = m_\nu$, while $(k_3)_{\max}$ is given by equation (3.49). Furthermore, we have $(E_3)_{\min} = 0$, while $(E_3)_{\max}$ is given by equation (3.48), and we have used the identity

$$\mathrm{d}k_3\, k_3 = \mathrm{d}E_3\, E_3, \qquad k_3 = \sqrt{E_3^2 + m_\nu^2}. \tag{3.51}$$

It is instructive to consider the double-differential energy loss d^2E_1, for a particle traveling at velocity $v_\nu \approx c$ (we restore factors of c for the moment), as it undergoes a decay with energy loss $E_1 - E_3$, due to the energy-resolved decay rate $(\mathrm{d}\Gamma/\mathrm{d}E)\,\mathrm{d}E$, in time $\mathrm{d}t = \mathrm{d}x/c$. It reads as follows,

$$\mathrm{d}^2 E_1 = -(E_1 - E_3)\,\frac{\mathrm{d}\Gamma}{\mathrm{d}E_3}\mathrm{d}E_3\,\frac{\mathrm{d}x}{c}. \tag{3.52}$$

Now we revert to natural units with $c = 1$, divide both sides of the equation by $\mathrm{d}x$ and integrate over the energy loss. One obtains

$$\frac{\mathrm{d}E_1}{\mathrm{d}x} = -\int \mathrm{d}E_3\,(E_1 - E_3)\,\frac{\mathrm{d}\Gamma}{\mathrm{d}E_3}. \tag{3.53}$$

Hence, the energy loss rate is obtained as

$$\frac{\mathrm{d}E}{\mathrm{d}x} = -\frac{G_{\mathrm{F}}^2}{4}\frac{1}{(2\pi)^4}\int_{(E_3)_{\min}}^{(E_3)_{\max}} \mathrm{d}E_3 \sqrt{E_3^2 + m_\nu^2}\,(E_1 - E_3)\int_{u_{\mathrm{th}}}^{1} \mathrm{d}u\;\mathcal{F}(E_1, E_3, u). \tag{3.54}$$

After a long, and somewhat tedious integration one finds the following expressions, which have been briefly indicated in [25],

$$\Gamma = \begin{cases} \dfrac{3}{2}\,\dfrac{G_{\mathrm{F}}^2\,m_\nu^5}{192\,\pi^3}\,\dfrac{m_\nu\,(E_1 - E_{\mathrm{th}})^2}{m_e^2\,E_{\mathrm{th}}} & E_1 \gtrapprox E_{\mathrm{th}} \\ \dfrac{2}{3}\,\dfrac{G_{\mathrm{F}}^2\,m_\nu^5}{192\pi^3}\,\dfrac{E_1}{m_\nu} & E_1 \gg E_{\mathrm{th}} \end{cases}, \tag{3.55a}$$

$$\frac{\mathrm{d}E}{\mathrm{d}x} = \begin{cases} 3\,\dfrac{G_{\mathrm{F}}^2\,m_\nu^5}{192\,\pi^3}\,\dfrac{(E_1 - E_{\mathrm{th}})^2}{E_{\mathrm{th}}} & E_1 \gtrapprox E_{\mathrm{th}} \\ \dfrac{4}{3}\,\dfrac{G_{\mathrm{F}}^2\,m_\nu^5}{192\pi^3}\,\dfrac{E_1^2}{m_\nu} & E_1 \gg E_{\mathrm{th}} \end{cases}. \tag{3.55b}$$

In the high-energy limit, one may rewrite the expressions as follows,

$$\Gamma = \frac{G_{\mathrm{F}}^2\,E_1^5\,\delta^2}{288\,\pi^3}, \qquad \frac{\mathrm{d}E}{\mathrm{d}x} = \frac{G_{\mathrm{F}}^2\,E_1^6\,\delta^2}{144\,\pi^3}, \qquad E_1 \gg E_{\mathrm{th}}. \tag{3.56}$$

The ratio of the energy loss rate to the decay rate is given as

$$\frac{1}{\Gamma}\,\frac{\mathrm{d}E}{\mathrm{d}x} = \begin{cases} 2\,\dfrac{m_e^2}{m_\nu} \approx E_{\mathrm{th}} & E_1 \geqslant E_{\mathrm{th}} \\ 2E_1 & E_1 \gg E_{\mathrm{th}} \end{cases}. \tag{3.57}$$

Here, according to equation (2.4), the threshold energy is

$$E_{\mathrm{th}} = (E_1)_{\mathrm{th}} = \sqrt{(k_1)_{\mathrm{th}}^2 - m_\nu^2} = 2\,\frac{m_e}{m_\nu}\,\sqrt{m_e^2 + m_\nu^2} \approx 2\,\frac{m_e^2}{m_\nu}. \tag{3.58}$$

For all results given in equations (3.55)–(3.57), we have assumed that $m_e \gg m_\nu$. Interpolating formulas are given as

$$\begin{aligned} \Gamma &\approx \frac{G_{\mathrm{F}}^2\,m_\nu^6}{128\,\pi^3\,m_e^2}\,\frac{(E_1 - E_{\mathrm{th}})^2}{E_{\mathrm{th}}}\left(1 + \frac{9m_\nu^2}{4m_e^2}\,\frac{E_1 - E_{\mathrm{th}}}{E_{\mathrm{th}}}\right)^{-1}, \\ \frac{\mathrm{d}E}{\mathrm{d}x} &\approx \frac{G_{\mathrm{F}}^2 m_\nu^5}{64\pi^3}\,\frac{(E_1 - E_{\mathrm{th}})^2}{E_{\mathrm{th}}}\left(\frac{4E_1E_{\mathrm{th}}}{4E_{\mathrm{th}}^2 + 9m_\nu(E_1 - E_{\mathrm{th}})}\right). \end{aligned} \tag{3.59}$$

These formulas interpolate between the regimes $E_1 \gtrapprox E_{\mathrm{th}}$ and $E_1 \gg E_{\mathrm{th}}$ given in equation (3.55).

4. Neutrino pair Cerenkov radiation

4.1. Preliminary steps

Having laid out the formalism in section 3, we can be brief in the current section. In the lab frame, again, the decay rate evaluates to

$$\Gamma = \frac{1}{2E_1} \int \frac{\mathrm{d}^3 p_3}{(2\pi)^3\, 2E_3} \left(\int \frac{\mathrm{d}^3 p_2}{(2\pi)^3\, 2E_2} \int \frac{\mathrm{d}^3 p_4}{(2\pi)^3\, 2E_4} \times (2\pi)^4\, \delta^{(4)}(p_1 - p_3 - p_2 - p_4) \left[\widetilde{\sum}_{\text{spins}} |\mathcal{M}|^2 \right] \right). \tag{4.1}$$

Here, $\widetilde{\sum}_{\text{spins}}$ refers to the specific way in which the average over the oncoming helicity states, and the outgoing helicities, needs to be carried out for tachyons [25]. We use the Lagrangian (3.3). The effective four-fermion interaction thus is

$$\mathcal{L} = \frac{G_{\mathrm{F}}}{2\sqrt{2}} [\overline{\nu}\, \gamma^\mu (1 - \gamma^5)\, \nu] [\overline{\nu}\, \gamma^\mu (1 - \gamma^5)\, \nu]. \tag{4.2}$$

The matrix element $\mathcal{M}$ evaluates to

$$\mathcal{M} = \frac{G_{\mathrm{F}}}{2\sqrt{2}} [\overline{u}^{\mathcal{T}}(p_3)\, \gamma_\lambda\, (1 - \gamma^5)\, u^{\mathcal{T}}(p_1)] [\overline{u}^{\mathcal{T}}(p_4)\, \gamma^\lambda\, (1 - \gamma^5)\, v^{\mathcal{T}}(p_2)], \tag{4.3}$$

in the notation for the tachyonic bispinors adopted previously. We use, again, the helicity-projected sum rule

$$\begin{aligned} \sum_\sigma u_\sigma^{\mathcal{T}}(p) \otimes \overline{u}_\sigma^{\mathcal{T}}(p) &= (-\vec{\Sigma} \cdot \hat{k})\, (\not{p} - \gamma^5\, m_\nu)\, \gamma^5 = -\gamma^5\, \gamma^0\, \gamma^i\, \hat{k}^i\, (\not{p} - \gamma^5\, m_\nu)\, \gamma^5 \\ &= -\not{\tau}\, \gamma^5\, \not{k}\, (\not{p} - \gamma^5\, m_\nu)\, \gamma^5, \end{aligned} \tag{4.4}$$

where $\tau = (1, 0, 0, 0)$ is a time-like unit vector. This leads to

$$\begin{aligned} &\frac{1}{2}(1 - \vec{\Sigma} \cdot \hat{k}) \sum_\sigma u_\sigma^{\mathcal{T}}(\vec{k}) \otimes \overline{u}_\sigma^{\mathcal{T}}(\vec{k}) = u_{\sigma=-1}(p) \otimes \overline{u}_{\sigma=-1}(p) \\ &= \frac{1}{2}(1 - \not{\tau}\, \gamma^5\, \not{k})\, (\not{p} - \gamma^5\, m_\nu)\, \gamma^5. \end{aligned} \tag{4.5}$$

The squared and spin-summed matrix element for the tachyonic decay process thus is

$$\begin{aligned} \widetilde{\sum_{\text{spins}}} |\mathcal{M}|^2 = \frac{G_{\mathrm{F}}^2}{8} \mathrm{Tr} \Bigg[& \frac{1}{2}(1 - \not{\tau}\, \gamma^5 \not{k}_3)\, (\not{p}_3 - \gamma^5\, m_\nu)\, \gamma^5\, \gamma_\lambda\, (1 - \gamma^5) \\ & \times \frac{1}{2}(1 - \not{\tau}\, \gamma^5\, \not{k}_1)\, (\not{p}_1 - \gamma^5\, m_\nu)\, \gamma^5\, \gamma_\nu\, (1 - \gamma^5) \Bigg] \\ & \times \mathrm{Tr} \Bigg[\frac{1}{2}(1 - \not{\tau}\, \gamma^5 \not{k}_4)\, (\not{p}_4 - \gamma^5\, m_\nu)\, \gamma^5\, \gamma^\lambda (1 - \gamma^5) \\ & \times \frac{1}{2}(1 - \not{\tau}\, \gamma^5 \not{k}_2)\, (\not{p}_2 + \gamma^5\, m_\nu)\, \gamma^5\, \gamma_\lambda (1 - \gamma^5) \Bigg]. \end{aligned} \tag{4.6}$$

Again, we have chosen the convention to denote the by p_2 the momentum of the outgoing antiparticle.

4.2. Integration and results

We now turn to the integration over the four-momenta of the outgoing particles. In the calculation, one may use the fact that the helicity projector is well approximated equal to the chirality projector for tachyonic particle in the high-energy limit (with the energy being significantly larger than the tachyonic mass). On the tachyonic mass shell, one has $p_1^2 = p_2^2 = p_3^2 = p_4^2 = -m_\nu^2$. The trace over the Dirac γ matrices can be evaluated with standard computer algebra [54, 55] and is inserted into equation (3.26). The d^3p_2 and d^3p_4 integrals are carried out with the help of the formulas (B.1*a*)–(B.1*c*), under the appropriate replacement $m_e^2 \to -m_\nu^2$. After the d^3p_2 and d^3p_4 integrations, we are left with an expression of the form

$$\Gamma = \frac{G_F^2}{8} \frac{1}{(2\pi)^5} \int_{q^2 > 4m_e^2} \frac{d^3p_3}{2E_3} \, \overline{\mathcal{F}}(p_1, p_3), \tag{4.7}$$

where

$$\overline{\mathcal{F}}(p_1, p_3) = \int \frac{d^3p_2}{2E_2} \int \frac{d^3p_4}{2E_4} \delta^{(4)}(p_1 - p_2 - p_3 - p_4) \, \overline{\mathcal{S}}(p_1, p_2, p_3, p_4). \tag{4.8}$$

The expressions for $\overline{\mathcal{S}}(p_1, p_2, p_3, p_4)$ as well as $\overline{\mathcal{F}}(p_1, p_3)$ are too lengthy to be displayed in the context of the current paper. We assume the same kinematics as in equations (3.42) and (3.43). The integrations are done with under the conditions that all $0 < E_3 < E_1$, and all $q^2 = (p_2 + p_4)^2$ for the pair are allowed (see equation (2.10)), leading to

$$\begin{aligned} \Gamma &= \frac{G_F^2}{8} \frac{1}{(2\pi)^5} \int_0^{2\pi} d\varphi \int_{k_3 = m_\nu}^{k_{\max}} \frac{dk_3 \, k_3^2}{2E_3} \int_{-1}^{1} du \, \overline{\mathcal{F}}(E_1, E_3, u) \\ &= \frac{G_F^2}{16} \frac{1}{(2\pi)^4} \int_0^{E_1} dE_3 \sqrt{E_3^2 + m_\nu^2} \int_{-1}^{1} du \, \overline{\mathcal{F}}(E_1, E_3, u), \end{aligned} \tag{4.9}$$

in full analogy with equation (2.10). Finally, the energy loss rate is obtained in full analogy with equation (3.54),

$$\frac{dE}{dx} = -\frac{G_F^2}{4} \frac{1}{(2\pi)^4} \int_0^{E_1} dE_3 \sqrt{E_3^2 + m_\nu^2} \, (E_1 - E_3) \int_{-1}^{1} du \, \mathcal{F}(E_1, E_3, u). \tag{4.10}$$

After rather tedious integration one finds the following expressions,

$$\Gamma = \frac{1}{3} \frac{G_F^2 \, m_\nu^4}{192\pi^3} E_1, \tag{4.11a}$$

$$\frac{dE_1}{dx} = \frac{1}{3} \frac{G_F^2 \, m_\nu^4}{192\pi^3} E_1^2. \tag{4.11b}$$

Strictly speaking, these formulas are valid only for $E_1 \gg m_\nu$, but this condition is easily fulfilled for all phenomenologically relevant neutrino energy, assuming that the modulus of neutrino masses $|m_\nu|$ does not exceed 1 eV. We reemphasize that, unlike in equation (3.55), there is no further threshold condition. Parametrically, the results in equations (3.55) and (4.11) are of the same order-of-magnitude. Hence, neutrino pair emission is the dominant decay channel in the medium-energy domain, for an oncoming tachyonic neutrino flavor eigenstate.

5. Phenomenological consequences

5.1. Decay processes on cosmic distance and time scales

If we assume that the tachyonic neutrino hypothesis is real, then a natural question to ask concerns the phenomenological consequences of the calculations outlined above. Parametrically, the decays by LPCR and NPCR described by equations (3.55) and (4.11) might set important limits on the observability of tachyonic neutrinos, provided the absolute magnitude of the decay energy loss rates are sufficiently large in order to induce a significant decay probability for neutrinos traveling across the Universe. This is because neutrinos registered by IceCube have to 'survive' the possibility of energy loss by decay, and if they are tachyonic, then lepton and NPCR processes become kinematically allowed.

Indeed, it is known that even very small Lorentz-violating parameters in a Lorentz-violating extension of the standard model may induce very significant energy loss processes at high energies [39, 40]. This is because at high energies, small violations of the Lorentz symmetry correspond to very high virtualities of the particles (kinematic deviations from the mass shell), and therefore, the magnitude of the Lorentz-violating parameters is in fact severely constrained by the 37 neutrinos with $E > 60\,\text{TeV}$ which are believed to be of cosmological origin and which have been registered by the IceCube collaboration [22, 23]. Meanwhile, preliminary evidence for a through-going muon depositing an energy of $\geqslant(2.6 \pm 0.3)\text{PeV}$ has been presented by some members of the IceCube collaboration [56]. The event could be interpreted in terms of a decay product of a neutrino of even higher energy [56]. (The difference of the energy deposited inside the detector and the neutrino energy, according to figure 4 of [23], is small.) If confirmed, this event would lead to even more restrictive bounds on the Lorentz-violating parameters.

The results given in equation (4.11) for the decay rate and energy loss rate due to NPCR are not subject to a threshold energy. Parametrically, they are of the same order-of-magnitude as those given for LPCR in equation (3.55), but the threshold energy is zero. Let us take as a typical cosmological distance 15 billion light years,

$$L = 15 \times 10^9\,\text{ly} = 1.42 \times 10^{26}\,\text{m} \tag{5.1}$$

and assume a (relative large) neutrino mass parameter of $m_0 = 10^{-2}\,\text{eV}$. One obtains for the relative energy loss according to equation (4.11*a*),

$$\frac{L}{E_1}\,\frac{\text{d}E_1}{\text{d}x} = \frac{1}{3}\,\frac{G_\text{F}^2\,m_0^4}{192\pi^3}\,E_1\,L = 5.02 \times 10^{-20}\,\frac{E_1}{\text{MeV}}. \tag{5.2}$$

Even at the large 'Big Bird' energy of $E_\nu \approx 2\,\text{PeV}$, the relative energy loss over 15 billion light years does not exceed 5×10^{-20}.

Again, assuming that $m_\nu = 10^{-2}\,\text{eV}$, one obtains for the decay rate the result

$$\Gamma = \frac{1}{3}\,\frac{G_\text{F}^2\,m_0^4}{192\pi^3}\,E_1 = 1.06 \times 10^{-37}\left(\frac{E_1}{\text{MeV}}\right)\left(\frac{\text{rad}}{\text{s}}\right). \tag{5.3}$$

Even for $E_\nu \approx 2\,\text{PeV}$, this means that the decay rate is only of order $10^{-28}\,\frac{\text{rad}}{\text{s}}$, corresponding to a lifetime of $\sim 10^{20}$ years, far exceeding the age of the Universe. Within the tachyonic model, quite surprisingly, both LPCR as well as NPCR are phenomenologically irrelevant, even for the highest-energy neutrinos registered by IceCube.

5.2. Neutrino mass and flavor eigenstates

The tachyonic Dirac equation [1, 6] reads as

$$(\mathrm{i}\gamma^\mu\partial_\mu - \gamma^5 m_\nu)\psi(x) = 0, \qquad (\mathrm{i}\gamma^\mu p_\mu - \gamma^5 m_\nu)u^{\mathcal{T}}(p) = 0, \tag{5.4}$$

where the latter form holds for the plane-wave ansatz $\psi(x) = u^{\mathcal{T}}(p)\exp(-\mathrm{i}p\cdot x)$. The bispinor solutions $u^{\mathcal{T}}(p)$ have been discussed at length in [6, 9] and are used here in equations (3.30) and (4.3). They apply, first and foremost, to a mass eigenstate, with a definite tachyonic mass parameter. The Fermi couplings are universal among all neutrino flavors, and hence, the interaction Lagrangians used in our paper share this property. Our results (3.55) and (4.11) for the decay and energy loss rates thus apply, at face value, to an incoming neutrino mass eigenstate. The results are thus relevant to the non-sterile neutrino flavor if at least one of the three observed non-sterile neutrino mass eigenstates is tachyonic.

We recall that the flavor eigenstates ν_f are connected to the mass eigenstates m_i by the Pontecorvo–Maki–Nakagawa–Sakata matrix,

$$m^2(\nu_f) = \sum_{i=1}^{3} |U_{fi}|^2\, m_i^2, \tag{5.5}$$

where U_{fi} denote the elements of the flavor-mass mixing matrix. The decay and energy loss rates of the flavor eigenstates are given as

$$\Gamma(\nu_f) = \sum_{i=1}^{3} |U_{fi}|^2\, \Gamma(m_i), \tag{5.6}$$

$$\frac{\mathrm{d}E}{\mathrm{d}x}(\nu_f) = \sum_{i=1}^{3} |U_{fi}|^2\, \frac{\mathrm{d}E}{\mathrm{d}x}(m_i). \tag{5.7}$$

For a slower-than light mass eigenstate i, one sets $\Gamma(m_i)$ and $\frac{\mathrm{d}E}{\mathrm{d}x}(m_i)$ to zero. Here, just to be pedantic, we should point out that the calculation of NPCR in this case has to be modified to include all tachyonic mass eigenstates in the exit channel, conceivably modifying the overall results as much as by adding a multiplicative factor three (if all mass eigenstates are available in the exit channel of the tachyonic NPCR decay, see figure 1(b)).

5.3. Lorentz invariance

The tachyonic dispersion relation $E^2 - \vec{k}^2 = -m_\nu^2$ conserves Lorentz invariance. Hence, one might ask about the Lorentz invariance of our results, and in particular, about the Lorentz invariance of the threshold condition (2.5); finally, one might 'chase' the high-energy neutrino, lowering its energy in the Lorentz-transformed, moving frame to a value below threshold. This question finds an answer in the subtleties of the tachyonic theory; we follow the discussion in [17]. Namely, upon a Lorentz transformation of the vacuum state, because there is no 'energy mass gap' between the positive- and negative-energy states, some of the annihilation operators of quantized fields will turn into creation operators, and vice versa. This point is explained in detail around equations (4.7)–(4.9) of [17]. (Incidentally, it is observed at the same place that the fundamental creation and annihilation operators of tachyonic fields have to be quantized according to fermionic statistics, which is another argument in favor of spin-1/2 rather than spinless tachyonic theories.) Furthermore, around equation (5.7) of [17], it is argued that the vacuum state in a tachyonic theory cannot be Lorentz-invariant, but is filled with those (real) anti-fermions whose energies are 'pushed down' to energies below zero, from initially positive-energy states, under the Lorentz

transformation. Our figure 2 illustrates how the decay and energy loss rates, under a Lorentz transformation, turn into neutrino–antineutrino collision rates (leading to decay and energy loss) with the 'downshifted' real antiparticle states which are the result of the Lorentz transformation, finally restoring the Lorentz invariance of the results for the decay and energy loss rates, given in equations (3.55) and (4.11).

5.4. Superluminal signal propagation

A very important question regarding the conceivable existence of tachyonic neutrinos concerns the possibility of superluminal signal propagation. We thus follow appendix A of [47] and ask how difficult it is to reliably 'stamp' any information onto the superluminal neutrinos. When assuming the dispersion relation $E = (\vec{k}^2 - m_\nu^2)^{1/2}$ with its classical equivalent $E = m_\nu \big/ \sqrt{v_\nu^2 - 1} = 0$, the dilemma is that high-energy tachyonic neutrinos approach the light cone and travel only infinitesimally faster than light itself. In the high-energy limit, their interaction cross sections may be sufficiently large to allow for good detection efficiency but this is achieved at the cost of sacrificing the 'speed advantage' in comparison to the speed of light. Low-energy tachyonic neutrinos may a substantially faster than light, but their interaction cross sections are small and the information sent via them may be lost. The smallness of the cross sections sets important boundaries for the possibility to transmit information, as follows. In Appendix A of [47], it has been shown that, by postulating that superluminal particles should not have the capacity to transport any 'imprinted' information into the past, one is naturally led to the assumption that any conceivable superluminal particles have to be very light, and weakly interacting.

Following figure 1 of [57] (see also [58]), we now supplement these considerations with a numerical estimate. Neutrino-electron cross sections for $1\,\text{GeV} < E_\nu < 1\,\text{PeV}$ can be estimated to good accuracy using the formula

$$\sigma = A_0 \, \frac{E_\nu}{E_0}, \tag{5.8}$$

with $A_0 \sim 0.0095\,\text{fb}$ and $E_0 = 1\,\text{GeV}$. By order-of-magnitude, equation (5.8) remains valid for neutrino scattering off electrons, for all three neutrino flavors, even if additional charged-current interactions exist for electron neutrinos, due to exchange graphs with virtual W bosons (for muon and tau neutrinos, only the Z boson contributes at tree level). A particle typically cannot be localized to better than an area equal to the square of its (reduced) Compton wavelength (we temporarily restore factors of $\hbar$ and c),

$$A_{\text{min}} = \lambda\!\!\!^{-2} = \left(\frac{\hbar}{m_\nu \, c} \right)^2. \tag{5.9}$$

The detection probability P for a perfectly focused particle therefore cannot exceed

$$P = \frac{\sigma}{A_{\text{min}}^2} = \frac{A_0 \, c^4 \, m_\nu^3}{E_0 \, \hbar^2} \sqrt{\frac{1}{\delta_\nu}}. \tag{5.10}$$

If we are to send information reliably, then the detection probability should be of order unity. Setting $P = 1$ leads to

$$\delta_\nu = \frac{A_0^2 \, c^8 \, m_\nu^6}{E_0^2 \, \hbar^4}. \tag{5.11}$$

When traveling at a speed $c + \delta c$ for a path length s, the neutrino acquires a path length difference of δs, which compares to its Compton wavelength $\lambda\!\!\!^{-} = \hbar/(m_\nu\, c)$ as follows,

$$\delta s = s\,\frac{\delta c}{c} = s\,\frac{\delta_\nu}{2}. \tag{5.12}$$

The distance traveled by the superluminal neutrino exceeds the distance traveled by a light beam by an amount $\delta s = \lambda\!\!\!^{-}$ when $s = s_0$ where

$$s_0 = \frac{2\,E_0^2\,\hbar^5}{A_0^2\,c^9\,m_\nu^7} = 6.63 \times 10^{74}\,\mathrm{m}\left(\frac{m_\nu}{\mathrm{eV}/c^2}\right)^{-7}. \tag{5.13}$$

Even at a (larger-than-realistic) mass square $m_\nu^2 = 1\,\mathrm{eV}^2$ for the tachyonic neutrino flavor eigenstate, the value of $s_0 \sim 10^{74}\,\mathrm{m}$ far exceeds the commonly assumed size of the Universe of $10^{26}\,\mathrm{m}$ by many orders of magnitude. The permissibility of slightly superluminal propagation on small length and distance scales has been discussed in the literature previously (see, e.g., [59]). Furthermore, we refer to the experiments in the group of Nimtz [60–62], which also use a compact apparatus and rely on the quantum mechanical tunneling effect, which lies outside the regime of classical mechanics. Thus, a very slightly superluminal neutrino flavor eigenstate with a light mass does not necessarily lead to a detectable violation of causality.

6. Conclusions

In the current article, we have considered the tachyonic neutrino decay width against lepton-pair and neutrino-pair Cerenkov radiation (LPCR and NPCR, see figure 1), via the exchange of a virtual Z^0 boson. This process is kinematically allowed for a fast-than-light, oncoming neutrino. We use the hypothesis of tachyonic neutrinos described by the tachyonic Dirac (not Majorana) equation [1–5]. Various kinematic considerations are summarized in section 2. The tachyonic threshold is found according to equation (2.5), $E_{\mathrm{th}} \approx 2m_e^2/m_\nu$, in the limit $m_e \gg m_\nu$. Specificities of the tachyonic decay are studied in section 2.1 (threshold calculation), section 2.2 (absence of threshold for NPCR), section 2.3 (maximum q^2 of the Z^0 boson and validity of Fermi theory), and section 2.4 (rest frame of the tachyon). In section 2.5, it is shown that, because tachyonic particle states may transform into antiparticle states upon a Lorentz transformation, it is indispensable to carry out the calculation directly in the lab frame [17, 18].

We continue with a discussion of the interaction Lagrangians relevant for our studies, from the GWS (Glashow–Weinberg–Salam) model in section 3.1. After a brief digression on the degrees of freedom of three-particle decay processes in section 3.2 and a discussion on the general rationale of the investigation in section 3.3, the calculation of the tachyonic decay width is approached in two steps. In section 3.4, we first demonstrate that it is possible to carry out standard decay rate calculations of the electroweak theory, directly in the lab frame, using the muon decay width as an example. We are finally in the position (see section 3.5) to carry out the integration of the decay rate, for the tachyonic dispersion relation, in the lab frame. We find an explicit dependence of the formulas for the decay rate, Γ, and the energy loss rate, $\mathrm{d}E/\mathrm{d}x$, on the energy E_1 of the incoming neutrino (all decay processes are studied within the conventions from figure 4). The main results of our investigations are summarized in equations (3.55)–(3.57); these formulas describe the decay width of a tachyonic neutrino against LPCR, and the energy loss per distance of an incoming tachyonic neutrino beam. This

investigation is supplemented, in section 4, by a calculation of NPCR, culminating in the results given in equation (4.11) for the decay and energy loss rates.

In section 5, we find that the NPCR process, even if threshold-less, has such a low probability due to the weak-interaction physics involved, that it cannot constrain the tachyonic models, even for large tachyonic neutrino mass parameters of the order of 10^{-2} eV. The lifetime of a tachyonic neutrino against LPCR and NPCR, assuming a realistic magnitude of the mass parameter, far exceeds the age of the Universe. Even a 'Big Bird' neutrino of energy of $E_\nu \approx 2$ PeV, would easily survive the travel from the blazar PKS B1424-418 (see [63]). In contrast to Lorentz-violating models, NPCR does not pressure the tachyonic neutrino hypothesis.

According to section 5, we should take the opportunity to clarify that in contrast to [25], it is actually impossible to relate a hypothetical cutoff of the cosmic neutrino spectrum at the 'Big Bird' energy of 2PeV to the threshold energy for (charged) LPCR, and thus, to a neutrino mass parameter. The reasons are twofold: first, a further decay process exists for tachyonic neutrinos which is not subject to a threshold condition, namely NPCR. Second, the decay and energy loss rates for *both* (charged) lepton as well as NPCR simply are too small to lead to any appreciable energy loss for an oncoming tachyonic neutrino flavor eigenstate, over cosmic distances and time scales. Formulated differently, we can say that that neither lepton nor NPCR processes pressure the tachyonic model in any way.

Finally, we hope that the detailed outline of the calculation of the decay processes given in sections 3 and 4 could be of interest in a wider context, regarding decay processes and cross sections involving tachyonic spin-1/2 particles. It is indispensable to introduce further helicity projectors in the calculation of the bispinor matrix elements relevant to the process, and the calculations become a little more complex than for ordinary Dirac spinors (see equations (3.33)–(3.35)). Our approach relies on a consistent formalism developed for the fundamental tachyonic bispinor solutions, as reported in various recent investigations [6–10].

Acknowledgments

Helpful conversation with J H Noble and B J Wundt are gratefully acknowledged. This research was supported by the National Science Foundation (Grant PHY-1403973 and PHY-1710856). This work was also supported by a János Bolyai Research Scholarship of the Hungarian Academy of Sciences.

Appendix A. Interaction terms in electroweak theory

From equation (12.240) of [50], we have for the combined interaction of the left-handed and right-handed fermionic currents with the W and Z bosons, and the electromagnetic A field, the following Lagrangian,

$$\begin{aligned}\mathcal{L}_\ell =\;& \bar{L}_e \,\mathrm{i}\,\gamma^\mu\,\partial_\mu\, L_e + \bar{e}_R\,\mathrm{i}\,\gamma^\mu\,\partial_\mu\, e_R \\ &+ \frac{g_w}{\sqrt{2}}(\bar{\nu}_e\,\gamma^\mu\,\mathrm{W}^+_\mu\, e_L + \bar{e}_L\,\gamma^\mu\,\mathrm{W}^-_\mu\,\nu_e) - g_w\,\sin\theta_\mathrm{W}\,\bar{e}\,\gamma^\mu\,A_\mu\,e \\ &- \frac{g_w}{2\cos\theta_\mathrm{W}}\,\bar{\nu}_e\,\gamma^\mu\,Z_\mu\,\nu_e + \frac{g_w}{2}\frac{\cos(2\theta_\mathrm{W})}{\cos\theta_\mathrm{W}}\,\bar{e}_L\,\gamma^\mu\,Z_\mu\,e_L - g_w\,\frac{\sin^2(\theta_\mathrm{W})}{\cos\theta_\mathrm{W}}\,\bar{e}_R\,\gamma^\mu\,Z_\mu\,e_R.\end{aligned} \tag{A.1}$$

Here, the subscripts L and R denote the left- and right-handed chirality components, e (as a mathematical symbol, not subscript) denotes the electron–positron field operator, the weak

coupling constant is g_w, and $\theta_{\rm W}$ is the Weinberg angle. One immediately reads off the electromagnetic Lagrangian $\mathcal{L}_1$ given in equation (3.1). Using $e_L = [(1 - \gamma^5)/2]e$, the coupling of the left-handed fermion currents to the W boson gives

$$\mathcal{L}_2 = \frac{g_w}{\sqrt{2}}(\bar\nu_e\,\gamma^\mu\,W_\mu^+\,e_L + \bar e_L\,\gamma^\mu\,W_\mu^-\,\nu_e) = \frac{g_w}{2\sqrt{2}}\,\bar e\,\gamma^\mu\,W_\mu^-\,(1-\gamma^5)\nu_e + \text{h.c.}, \tag{A.2}$$

which is just $\mathcal{L}_2$ (see equation (3.2)). The coupling term of the neutrino to the Z boson can be read off as

$$\mathcal{L}_3 = -\frac{g_w}{2\cos\theta_{\rm W}}\,\bar\nu_e\,\gamma^\mu\,Z_\mu\,\nu_e = -\frac{g_w}{4\cos\theta_{\rm W}}\,\bar\nu_e\,\gamma^\mu\,(1-\gamma^5)\,Z_\mu\,\nu_e, \tag{A.3}$$

where we take into account that ν_e is equal to its left-handed chirality component (see equation (3.3)). The only term which requires a little work is the interaction of the electron current with the Z boson,

$$\begin{aligned}
\mathcal{L}_4 &= \frac{g_w}{2}\frac{\cos(2\theta_{\rm W})}{\cos\theta_{\rm W}}\,\bar e_L\,\gamma^\mu\,Z_\mu\,e_L - g_w\,\frac{\sin^2(\theta_{\rm W})}{\cos\theta_{\rm W}}\,\bar e_R\,\gamma^\mu\,Z_\mu\,e_R \\
&= \frac{g_w}{2}\frac{1-2\sin^2(\theta_{\rm W})}{\cos\theta_{\rm W}}\,\bar e_L\,\gamma^\mu\,Z_\mu\,e_L - g_w\,\frac{\sin^2(\theta_{\rm W})}{\cos\theta_{\rm W}}\,\bar e_R\,\gamma^\mu\,Z_\mu\,e_R \\
&= \frac{g_w}{2}\frac{1}{\cos\theta_{\rm W}}\,\bar e\,\gamma^\mu\,\frac{1-\gamma^5}{2}Z_\mu\,e - g_w\,\frac{\sin^2(\theta_{\rm W})}{\cos\theta_{\rm W}}\,Z_\mu\left\{\bar e\,\gamma^\mu\frac{1-\gamma^5}{2}\,e + \bar e\,\gamma^\mu\,\frac{1+\gamma^5}{2}\,e\right\} \\
&= \frac{g_w}{2\cos\theta_{\rm W}}\,\bar e\left[\frac{1}{2}\,\gamma^\mu(1-\gamma^5) - 2\sin^2(\theta_{\rm W})\,\gamma^\mu\right]e\,Z_\mu \\
&= -\frac{g_w}{2\cos\theta_{\rm W}}\,\bar e\left[\left(-\frac{1}{2} + 2\sin^2(\theta_{\rm W})\right)\gamma^\mu + \frac{1}{2}\,\gamma^\mu\,\gamma^5\right]e\,Z_\mu. \\
&= -\frac{g_w}{2\cos\theta_{\rm W}}\,\bar e\,[c_{\rm V}\,\gamma^\mu - c_{\rm A}\,\gamma^\mu\,\gamma^5]\,e\,Z_\mu,
\end{aligned} \tag{A.4}$$

where

$$c_{\rm V} = -\frac{1}{2} + 2\sin^2(\theta_{\rm W}), \qquad c_{\rm A} = -\frac{1}{2}. \tag{A.5}$$

This result also is in agreement with equation (5.57) on p 153 of [64], up to an overall minus sign which is fixed by the conventions. According to p 107 of [65], the effective Weinberg angle reads as

$$\sin^2\theta_{\rm W} = 0.23146(12), \qquad \sin^2\theta_{\rm W} \approx 0.25, \tag{A.6}$$

which justifies the approximation $c_{\rm V} \approx 0$, and $c_{\rm A} \approx -1/2$. This approximation is often used in the literature (see the remark preceding equation (2) of [31] and p 153 of [64]). We also quote from [31] the W boson mass,

$$M_W = (80.385 \pm 0.015)\,\frac{\rm GeV}{c^2} = 80.385(15)\,\frac{\rm GeV}{c^2} \tag{A.7}$$

and the Z boson mass

$$M_Z = (91.1876 \pm 0.0021)\,\frac{\rm GeV}{c^2} = 91.1876(21)\,\frac{\rm GeV}{c^2}. \tag{A.8}$$

The W and Z masses are connected by virtue of the Weinberg angle, according to equation (3.5).

Appendix B. Covariant pair production integrals

In our evaluation, for the outgoing electron–positron pair in the decay of the tachyonic neutrino, we shall need a few integrals. In the conventions of figure 1, the outgoing momenta p_2 and p_4 are on the mass shell, $E_2 = \sqrt{\vec{k}_2^{\,2} + m_e^2}$ and $E_4 = \sqrt{\vec{k}_4^{\,2} + m_e^2}$. Let us anticipate the results for the integrals I, J, and K, which are defined as follows,

$$I(q) = \int \frac{\mathrm{d}^3 p_2}{2E_2} \int \frac{\mathrm{d}^3 p_4}{2E_4} \delta^{(4)}(q - p_2 - p_4) = \frac{\pi}{2} \sqrt{1 - \frac{4\,m_e^2}{q^2}}, \tag{B.1a}$$

$$\begin{aligned} J_{\lambda\rho}(q) &= \int \frac{\mathrm{d}^3 p_2}{2E_2} \int \frac{\mathrm{d}^3 p_4}{2E_4} \delta^{(4)}(q - p_2 - p_4)(p_{2\lambda}\, p_{4\rho}) \\ &= \sqrt{1 - \frac{4\,m_e^2}{q^2}} \left[g_{\lambda\rho}\, \frac{\pi}{24}(q^2 - 4m_e^2) + q_\lambda\, q_\rho\, \frac{\pi}{12} \left(1 + \frac{2m_e^2}{q^2} \right) \right], \end{aligned} \tag{B.1b}$$

$$K(q) = \int \frac{\mathrm{d}^3 p_2}{2E_2} \int \frac{\mathrm{d}^3 p_4}{2E_4} \delta^{(4)}(q - p_2 - p_4)(p_2 \cdot p_4) = \frac{\pi}{4} \sqrt{1 - \frac{4\,m_e^2}{q^2}} (q^2 - 2m_e^2). \tag{B.1c}$$

By symmetry, one immediately has $J_{\rho\lambda}(q) = J_{\lambda\rho}(q)$. The evaluation of these integrals is essentially simplified because of the Lorentz invariance of the integration measures, which entails the possibility to choose a coordinate system where $q = (q^0, \vec{q} = \vec{0})$, and then, identify the occurrences of $(q^0)^2$ with q^2. The derivation of the results is discussed below. We observe that because $E_2 = \sqrt{\vec{k}_2^{\,2} + m_e^2}$ and $E_4 = \sqrt{\vec{k}_4^{\,2} + m_e^2}$, we have

$$\frac{\mathrm{d}E_4}{\mathrm{d}|\vec{k}_4|} = \frac{\mathrm{d}\sqrt{|\vec{k}|_4^2 + m_e^2}}{\mathrm{d}|\vec{k}_4|} = \frac{\frac{1}{2}\, 2|\vec{k}_4|}{\sqrt{|\vec{k}|_4^2 + m_e^2}} = \frac{|\vec{k}_4|}{E_4}, \qquad E_4\, \mathrm{d}E_4 = |\vec{k}_4|\, \mathrm{d}|\vec{k}_4|. \tag{B.2}$$

We shall go through the calculation if the integral $I(q)$ in great detail,

$$\begin{aligned} I(q) &= \int \frac{\mathrm{d}^3 p_2}{2E_2} \int \frac{\mathrm{d}^3 p_4}{2E_4}\, \delta^{(4)}(q - p_2 - p_4) \\ &= \int \frac{\mathrm{d}^3 p_2}{2E_2} \int \frac{\mathrm{d}^3 p_4}{2E_4}\, \delta^{(3)}(\vec{q} - \vec{k}_2 - \vec{k}_4)\, \delta(q_0 - E_2 - E_4) \\ &\overset{\vec{q} = \vec{0}}{=} \int \frac{\mathrm{d}^3 p_2}{2E_2} \int \frac{\mathrm{d}^3 p_4}{2E_4}\, \delta^{(3)}(-\vec{k}_2 - \vec{k}_4)\, \delta(q_0 - E_2 - E_4) = \int \frac{\mathrm{d}^3 p_4}{2E_4} \frac{1}{2E_4}\, \delta(q_0 - 2E_4) \\ &= 4\pi \int \frac{\mathrm{d}E_4\, E_4\, p_4}{4E_4^2} \Big(\tfrac{1}{2}\, \delta(E_4 - \tfrac{1}{2} q_0) \Big) = \frac{\pi}{2} \int \mathrm{d}E_4 \sqrt{\frac{E_4^2 - m_e^2}{E_4^2}}\, \delta\Big(E_4 - \tfrac{1}{2} q_0 \Big) \\ &= \frac{\pi}{2} \sqrt{\frac{q_0^2/4 - m_e^2}{q_0^2/4}} = \frac{\pi}{2} \sqrt{1 - \frac{4\,m_e^2}{q^2}}. \end{aligned} \tag{B.3}$$

For $J_{\lambda\rho}(q)$, we write

$$J_{\lambda\rho}(q) = \int \frac{\mathrm{d}^3 p_2}{2E_2} \int \frac{\mathrm{d}^3 p_4}{2E_4} \delta^{(4)}(q - p_2 - p_4)(p_{2\lambda}\, p_{4\rho}) = A\, q^2\, g_{\lambda\rho} + B\, q_\lambda\, q_\rho. \tag{B.4}$$

Projection onto the tensors $g^{\lambda\rho}$ and $q^\lambda\, q^\rho$ leads to

$$g^{\lambda\rho} J_{\lambda\rho}(q) = q^2(4A + B), \qquad q^\lambda\, q^\rho J_{\lambda\rho}(q) = q^4(A + B). \tag{B.5}$$

Now, we have

$$\begin{aligned}
g^{\lambda\rho} J_{\lambda\rho}(q) &= \int \frac{\mathrm{d}^3 p_2}{2E_2} \int \frac{\mathrm{d}^3 p_4}{2E_4}\, \delta^{(4)}(q - p_2 - p_4)(p_2 \cdot p_4) \\
\vec{q} &\underset{=}{=} \vec{0} \int \frac{\mathrm{d}^3 p_2}{2E_2} \int \frac{\mathrm{d}^3 p_4}{2E_4}\, \delta^{(3)}(-\vec{k}_2 - \vec{k}_4)\, \delta(q_0 - E_2 - E_4)(E_2\, E_4 - \vec{k}_2 \cdot \vec{k}_4) \\
&= \int \frac{\mathrm{d}^3 p_4}{2E_4} \frac{1}{2E_4}\, \delta(q_0 - 2E_4)(E_4^2 + \vec{k}_4^{\,2}) \\
&= \frac{4\pi}{4} \int \frac{\mathrm{d}E_4\, E_4\, |\vec{k}_4|}{E_4^2} \tfrac{1}{2}\, \delta\Big(E_4 - \tfrac{1}{2} q_0\Big)(E_4^2 + \vec{k}_4^{\,2}) \\
&= \pi \int \mathrm{d}E_4 \sqrt{\frac{E_4^2 - m_e^2}{E_4^2}}\, \tfrac{1}{2}\, \delta\Big(E_4 - \tfrac{1}{2} q_0\Big)(2E_4^2 - m_e^2) \\
&= \frac{\pi}{2} \sqrt{\frac{q_0^2/4 - m_e^2}{q_0^2/4}}\, (q_0^2/2 - m_e^2) \\
&= \frac{\pi}{4} \sqrt{1 - \frac{4\, m_e^2}{q^2}}\, (q^2 - 2m_e^2).
\end{aligned} \tag{B.6}$$

Yet,

$$\begin{aligned}
q^\lambda q^\rho J_{\lambda\rho}(q) &= \int \frac{\mathrm{d}^3 p_2}{2E_2} \int \frac{\mathrm{d}^3 p_4}{2E_4}\, \delta^{(4)}(q - p_2 - p_4)(q \cdot p_2)(q \cdot p_4) \\
\vec{q} &\underset{=}{=} \vec{0} \int \frac{\mathrm{d}^3 p_2}{2E_2} \int \frac{\mathrm{d}^3 p_4}{2E_4}\, \delta^{(3)}(-\vec{k}_2 - \vec{k}_4)\, \delta(q_0 - E_2 - E_4)(q_0\, E_2)(q_0\, E_4) \\
&= \int \frac{\mathrm{d}^3 p_4}{2E_4} \frac{1}{2E_4}\, \delta(q_0 - 2E_4)(q_0)^2\, E_4^2 \\
&= \frac{4\pi}{4} \int \frac{\mathrm{d}E_4\, E_4\, |\vec{k}_4|}{E_4^2} \tfrac{1}{2}\, \delta\Big(E_4 - \tfrac{1}{2} q_0\Big)(q_0)^2\, E_4^2 \\
&= \pi \int \mathrm{d}E_4 \sqrt{\frac{E_4^2 - m_e^2}{E_4^2}}\, \delta\Big(E_4 - \tfrac{1}{2} q_0\Big)(q_0)^2\, E_4^2 \\
&= \frac{\pi}{2} \sqrt{\frac{q_0^2/4 - m_e^2}{q_0^2/4}}\, \frac{q_0^4}{4} = \frac{\pi}{8} \sqrt{1 - \frac{4\, m_e^2}{q^2}}\, q^4.
\end{aligned} \tag{B.7}$$

Combining equations (B.5)–(B.7), one may finally solve for A and B,

$$A = \frac{\pi}{24\, q^2} \sqrt{1 - \frac{4\, m_e^2}{q^2}}\, (q^2 - 4m_e^2), \qquad B = \frac{\pi}{12\, q^2} \sqrt{1 - \frac{4\, m_e^2}{q^2}}\, (q^2 + 2m_e^2). \tag{B.8}$$

Thus, we confirm the result in equation (B.1*b*),

$$J_{\lambda\rho}(q) = g_{\lambda\rho}\,\frac{\pi}{24}\,\sqrt{1-\frac{4\,m_e^2}{q^2}}\,(q^2-4m_e^2) + q_\lambda\,q_\rho\,\frac{\pi}{12}\,\sqrt{1-\frac{4\,m_e^2}{q^2}}\left(1+\frac{2m_e^2}{q^2}\right). \tag{B.9}$$

Finally, contracting with the metric, one has

$$K(q) = g^{\lambda\rho}J_{\lambda\rho}(q) = \frac{\pi}{4}\,\sqrt{1-\frac{4\,m_e^2}{q^2}}\,(q^2-2m_e^2), \tag{B.10}$$

confirming the result in equation (B.1*c*).

References

[1] Chodos A, Hauser A I and Kostelecky V A 1985 *Phys. Lett.* B **150** 431
[2] Chodos A, Kostelecky V A, Potting R and Gates E 1992 *Mod. Phys. Lett.* A **7** 467
[3] Kostelecky V A 1993 Mass bounds for spacelike neutrinos *Topics on Quantum Gravity and Beyond: Essays in Honor of Louis Witten on his Retirement* ed F Mansouri and J J Scanio (Singapore: World Scientific)
[4] Chodos A and Kostelecky V A 1994 *Phys. Lett.* B **336** 295
[5] Chodos A 2012 Light cone reflection and the spectrum of neutrinos arXiv:1206.5974
[6] Jentschura U D and Wundt B J 2012 *Eur. Phys. J.* C **72** 1894
[7] Jentschura U D 2012 *J. Mod. Phys.* **3** 887
[8] Jentschura U D and Wundt B J 2012 *J. Phys. A: Math. Theor.* **45** 444017
[9] Jentschura U D and Wundt B J 2013 *ISRN High Energy Phys.* **2013** 374612
[10] Jentschura U D and Wundt B J 2014 *J. Phys. G: Nucl. Part. Phys.* **41** 075201
[11] Ciborowski J 1998 *Acta Phys. Pol.* B **29** 113
[12] Griffiths D 1987 *Introduction to Elementary Particles* (New York: Wiley)
[13] Bilaniuk O M P, Deshpande V K and Sudarshan E C G 1962 *Am. J. Phys.* **30** 718
[14] Arons M E and Sudarshan E C G 1968 *Phys. Rev.* **173** 1622
[15] Dhar J and Sudarshan E C G 1968 *Phys. Rev.* **174** 1808
[16] Bilaniuk O-M and Sudarshan E C G 1969 *Nature* **223** 386
[17] Feinberg G 1967 *Phys. Rev.* **159** 1089
[18] Feinberg G 1978 *Phys. Rev.* D **17** 1651
[19] Recami E 2009 *J. Phys.: Conf. Ser.* **196** 012020
[20] Bilaniuk O M 2009 *J. Phys.: Conf. Ser.* **196** 012021
[21] Bose S K 2009 *J. Phys.: Conf. Ser.* **196** 012022
[22] Aartsen M G *et al* (IceCube Collaboration) 2013 *Phys. Rev. Lett.* **111** 021103
[23] Aartsen M G *et al* (IceCube Collaboration) 2014 *Phys. Rev. Lett.* **113** 101101
[24] Botner O 2015 IceCube neutrino observatory: present and future *2015 IceCube Particle Astrophysics Symp. (Madison, WI, 4–6 May 2015)*
[25] Jentschura U D and Ehrlich R 2016 *Adv. High Energy Phys.* **2016** 4764981
[26] Recami E and Mignani R 1974 *Rivista Nuovo Cimento* **4** 209
[27] Maccarone G D and Recami E 1980 *Nuovo Cimento* **57** 85
[28] Chang T 2000 A new Dirac-type equation for tachyonic neutrinos arXiv:hep-th/0011087
[29] Chang T 2002 *Nucl. Sci. Technol.* **13** 129
[30] Chang T 2002 Parity violation and a preferred frame arXiv:quant-ph/0204002
[31] Cohen A G and Glashow S L 2011 *Phys. Rev. Lett.* **107** 181803
[32] Bi X-J, Yin P-F, Yu Z-H and Yuan Q 2011 *Phys. Rev. Lett.* **107** 241802
[33] Bezrukov F and Lee H M 2012 *Phys. Rev.* D **85** 031901(R)
[34] Diaz J S, Kostelecky V A and Mewes M 2014 *Phys. Rev.* D **89** 043005
[35] Diaz J 2014 *Adv. High. Energy Phys.* **2014** 962410
[36] Tasson J D 2014 *Rep. Prog. Phys.* **77** 062901
[37] Stecker F W, Scully S T, Liberati S and Mattingly D 2015 *Phys. Rev.* D **91** 045009
[38] Liberati S 2015 *J. Phys.: Conf. Ser.* **631** 012011
[39] Stecker F W and Scully S T 2014 *Phys. Rev.* D **90** 043012
[40] Stecker F W 2014 *Astropart. Phys.* **56** 16

[41] Mazon D 2014 *Phys. Rev.* D **89** 056012
[42] Mattingly D M, Maccione L, Galaverni M, Liberati S and Sigl G 2010 *J. Cosmol. Astropart. Phys.* **02** 007
[43] Flambaum V V and Pospelov M 2012 *Phys. Rev.* D **86** 107502
[44] Sazdovic B and Vasilic M 2013 *J. High Energy Phys.* **03** 047
[45] Hojman S A and Asenjo F A 2013 *Class. Quantum Grav.* **30** 025008
[46] Noble J H and Jentschura U D 2015 *Phys. Rev.* A **92** 012101
[47] Jentschura U D, Horváth D, Nagy S, Nándori I, Trócsányi Z and Ujvári B 2014 *Int. J. Mod. Phys.* E **23** 1450004
[48] Strumia A and Vissani F 2006 Neutrino masses and mixings and... arXiv:hep-ph/0606054
[49] Olive K A *et al* (Particle Data Group) 2014 *Chin. Phys.* C **38** 090001
[50] Itzykson C and Zuber J B 1980 *Quantum Field Theory* (New York: McGraw-Hill)
[51] Lahiri A and Pal P B 2011 *Quantum Field Theory* (Oxford: Alpha Science)
[52] John M 2011 *Lecture Notes of the Course on Particle Basics: lecture 5: Phase space and decay rates (unpublished) (Oxford)* (Oxford: Oxford University)
[53] Berestetskii V B, Lifshitz E M and Pitaevskii L P 1982 *Quantum Electrodynamics* (*Course on Theoretical Physics* vol 4) 2nd edn (Oxford: Pergamon)
[54] Hsieh A and Yehudai E 1992 *Comput. Phys.* **6** 253
[55] Wolfram S 1999 *The Mathematica Book* 4th edn (Cambridge: Cambridge University Press)
[56] Schoenen S and Raedel L 2015 see http://astronomerstelegram.org/?read=7856
[57] Formaggio J A and Zeller G P 2012 *Rev. Mod. Phys.* **84** 1307
[58] See the cross sections tabulated at http://cupp.oulu.fi/neutrino/nd-cross.html
[59] Aharonov Y, Reznik B and Stern A 1998 *Phys. Rev. Lett.* **81** 2190
[60] Enders A and Nimtz G 1992 *J. Phys.* I **2** 1693
[61] Nimtz G and Stahlhofen A A 2008 *Ann. Phys.* **17** 374
[62] Nimtz G 2009 *Found. Phys.* **39** 1346
[63] Kadler M *et al* 2016 *Nat. Phys.* **12** 807
[64] Horejsi J 2002 *Fundamentals of Electroweak Theory* (Prague: Karolinum Press)
[65] Beringer J *et al* (Particle Data Group) 2012 *Phys. Rev.* D **86** 010001